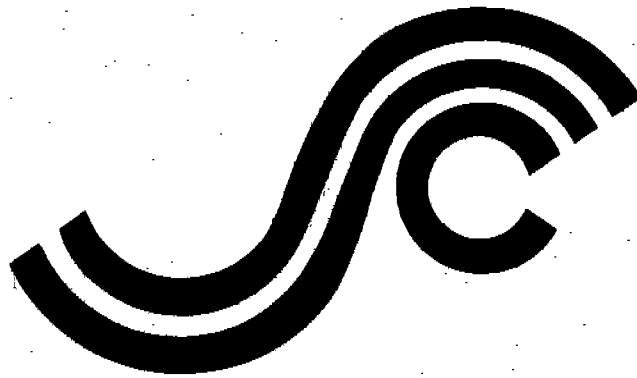


SSC-299

**ULTIMATE STRENGTH OF A
SHIP'S HULL GIRDER IN
PLASTIC AND BUCKLING MODES**



**This document has been approved
for public release and sale; its
distribution is unlimited.**

SHIP STRUCTURE COMMITTEE

1980

SHIP STRUCTURE COMMITTEE

The SHIP STRUCTURE COMMITTEE is constituted to prosecute a research program to improve the hull structures of ships and other marine structures by an extension of knowledge pertaining to design, materials and methods of construction.

RADM H. H. BELL (Chairman)
Chief, Office of Merchant Marine
Safety
U. S. Coast Guard

Mr. P. M. PALERMO
Deputy Director,
Hull Group
Naval Sea Systems Command

Mr. W. N. HANNAN
Vice President
American Bureau of Shipping

Mr. M. PITKIN
Assistant Administrator for
Commercial Development
Maritime Administration

Mr. R. B. KRAHL
Chief, Branch of Marine Oil
and Gas Operations
U. S. Geological Survey

Mr. C. J. WHITESTONE
Chief Engineer
Military Sealift Command

CDR T. H. ROBINSON, U.S. Coast Guard (Secretary)

SHIP STRUCTURE SUBCOMMITTEE

The SHIP STRUCTURE SUBCOMMITTEE acts for the Ship Structure Committee on technical matters by providing technical coordination for the determination of goals and objectives of the program, and by evaluating and interpreting the results in terms of structural design, construction and operation.

U.S. COAST GUARD

CAPT R. L. BROWN
CDR J. C. CARD
CDR J. A. SANIAL, JR.
CDR W. M. SIMPSON, JR.

NAVAL SEA SYSTEMS COMMAND

Mr. R. CHIU
Mr. R. JOHNSON
Mr. J. B. O'BRIEN

AMERICAN BUREAU OF SHIPPING

DR. D. LIU
MR. I. L. STERN

NATIONAL ACADEMY OF SCIENCES SHIP RESEARCH COMMITTEE

Mr. O. H. OAKLEY - Liaison
Mr. R. W. RUMKE - Liaison

THE SOCIETY OF NAVAL ARCHITECTS & MARINE ENGINEERS

Mr. N. O. HAMMER - Liaison

WELDING RESEARCH COUNCIL

Mr. K. H. KOOPMAN - Liaison

U. S. MERCHANT MARINE ACADEMY

Dr. C.-B. KIM - Liaison

MILITARY SEALIFT COMMAND

MR. G. ASHF
MR. T. W. CHAPMAN
MR. A. B. STAVOVY (Chairman)
MR. D. STEIN

U. S. GEOLOGICAL SURVEY

MR. R. J. GIANCEPELLI
MR. J. GREGORY

MARITIME ADMINISTRATION

MR. N. O. HAMMER
DR. W. MACLEAN
Mr. F. SEIBOLD
Mr. M. TOUMA

INTERNATIONAL SHIP STRUCTURES CONGRESS

Mr. S. G. STIANSEN - Liaison

AMERICAN IRON & STEEL INSTITUTE

Mr. R. H. STERNE - Liaison

STATE UNIVERSITY OF NEW YORK MARITIME COLLEGE

Dr. W. R. PORTER - Liaison

U. S. COAST GUARD ACADEMY

CAPT W. C. NOLAN - Liaison

U. S. NAVAL ACADEMY

Dr. R. BHATTACHARYA - Liaison

Member Agencies:

*United States Coast Guard
Naval Sea Systems Command
Military Sealift Command
Maritime Administration
United States Geological Survey
American Bureau of Shipping*



An Interagency Advisory Committee
Dedicated to Improving the Structure of Ships

Address Correspondence to:

Secretary, Ship Structure Committee
U.S. Coast Guard Headquarters, (G-M/TP 13)
Washington, D.C. 20593

SR-1262

JULY 1980

Knowledge of the ultimate strength of ships is important, particularly in determining the appropriate margins of safety or the possible risk of failure under the loads acting on the ship. While significant work had been done on determining hull girder ultimate strength under vertical bending moments, additional work was necessary to determine the strength under a combination of vertical, lateral and torsional loads.

The Ship Structure Committee undertook an investigation that would include an analytical prediction of elastic buckling, yielding, plastic buckling, and collapse under a variety of combined loads; experimental verification of the analytical prediction; and, finally, development of a prediction procedure.

The results of this study are presented in this report.

A handwritten signature in cursive script, appearing to read 'Henry H. Bell', is written over the printed name.

Henry H. Bell
Rear Admiral, U.S. Coast Guard
Chairman, Ship Structure Committee

1. Report No. SSC-299		2. Government Accession No.		3. Recipient's Catalog No.	
4. Title and Subtitle ULTIMATE STRENGTH OF A SHIP'S HULL GIRDER PLASTIC AND BUCKLING MODES				5. Report Date JUNE 1980	
				6. Performing Organization Code	
7. Author(s) A. E. Mansour and A. Thayamballi				8. Performing Organization Report No.	
9. Performing Organization Name and Address Mansour Engineering Inc. Berkeley, CA 94704				10. Work Unit No. (TRAVIS)	
				11. Contract or Grant No. DOT-CG-74755-A	
12. Sponsoring Agency Name and Address U.S. Coast Guard Office of Merchant Marine Safety Washington, D.C. 20593				13. Type of Report and Period Covered FINAL	
				14. Sponsoring Agency Code G-M	
15. Supplementary Notes					
16. Abstract Knowledge of the limiting conditions beyond which a ship's hull girder will fail to perform its function is important in assessing accurately the true margin of safety in the design of ships. Such information is essential also for developing design procedures, requirements, and rules which achieve uniform standards among vessels of different sizes and types. In this report, these limiting conditions were analyzed with the objective of determining the ultimate strength of a hull girder. The ship was considered to be subjected to a realistic loading consisting of vertical and lateral bending moments and torsional moment. Buckling and instability of the hull stiffened plates, the fully plastic yield moments, and the shakedown moments were further developed in a procedure for estimating the ultimate capacity of the hull. New interaction relations for the ultimate strength of ships subjected to combined moments were developed in this study. The fracture (fatigue and brittle) modes of failure were not included. An application to a 200,000 ton displacement tanker was carried out to show the details of the procedure and to examine the effects of various factors on the ultimate capacity of the hull. Lack of adequate formulations in certain areas were pointed out particularly when the collapse mode involved coupling between several mechanisms of failure. Analytical studies as well as a two-part test program were recommended with their objectives outlined.					
17. Key Words <i>ship hull girder instability</i> <i>ultimate strength</i> <i>buckling</i> <i>collapse</i> <i>combined loads</i>			18. Distribution Statement Document is available to the U.S. Public through the National Technical Information Service, Springfield, VA 22161		
19. Security Classif. (of this report) UNCLASSIFIED		20. Security Classif. (of this page) UNCLASSIFIED		21. No. of Pages 68	22. Price

METRIC CONVERSION FACTORS

Approximate Conversions to Metric Measures

Symbol	When You Know	Multiply by	To Find	Symbol
LENGTH				
in	inches	2.5	centimeters	cm
ft	feet	30	centimeters	cm
yd	yards	0.9	meters	m
mi	miles	1.6	kilometers	km
AREA				
in ²	square inches	6.5	square centimeters	cm ²
ft ²	square feet	0.09	square meters	m ²
yd ²	square yards	0.8	square meters	m ²
mi ²	square mile	2.6	square kilometers	km ²
	acres	0.4	hectares	ha
MASS (weight)				
oz	ounces	28	grams	g
lb	pounds	0.45	kilograms	kg
	short tons (2000 lb)	0.9	tonnes	t
VOLUME				
tsp	teaspoons	5	milliliters	ml
Tbsp	tablespoons	15	milliliters	ml
fl oz	fluid ounces	30	milliliters	ml
c	cups	0.24	liters	l
pt	pints	0.47	liters	l
qt	quarts	0.95	liters	l
gal	gallons	3.8	liters	l
ft ³	cubic feet	0.03	cubic meters	m ³
yd ³	cubic yards	0.76	cubic meters	m ³
TEMPERATURE (exact)				
°F	Fahrenheit temperature	5/9 (after subtracting 32)	Celsius temperature	°C

* 1 in = 2.54 (exactly). For other exact conversions and more detailed tables, see NBS Misc. Publ. 286, Units of Weights and Measures, Price \$2.25, SD Catalog No. C13.10-286.

Approximate Conversions from Metric Measures

Symbol	When You Know	Multiply by	To Find
LENGTH			
mm	millimeters	0.04	inches
cm	centimeters	0.4	inches
m	meters	3.3	feet
m	meters	1.1	yards
km	kilometers	0.6	miles
AREA			
cm ²	square centimeters	0.16	square inches
m ²	square meters	1.2	square yards
km ²	square kilometers	0.4	square miles
ha	hectares (10,000 m ²)	2.5	acres
MASS (weight)			
g	grams	0.035	ounces
kg	kilograms	2.2	pounds
t	tonnes (1000 kg)	1.1	short tons
VOLUME			
ml	milliliters	0.03	fluid ounces
l	liters	2.1	pints
l	liters	1.06	quarts
l	liters	0.26	gallons
m ³	cubic meters	35	cubic feet
m ³	cubic meters	1.3	cubic yards
TEMPERATURE (exact)			
°C	Celsius temperature	9/5 (then add 32)	Fahrenheit temperature

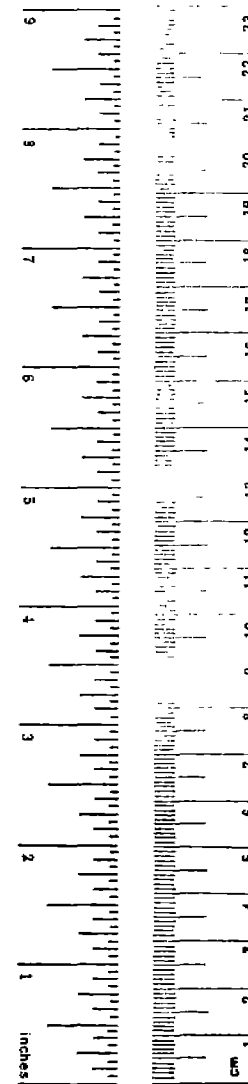
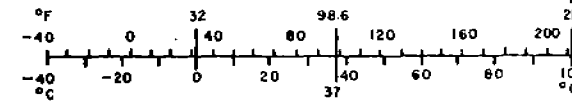


TABLE OF CONTENTS

	<u>Page</u>
I. INTRODUCTION	1
II. ULTIMATE STRENGTH UNDER VERTICAL MOMENT.	3
A. Identification of Possible Modes of Failure.	3
B. Evaluation of Failure Due to Yielding and Plastic Flow . .	3
C. Evaluation of Failure Due to Instability and Buckling. . .	12
III. ULTIMATE STRENGTH UNDER LATERAL MOMENT	19
A. Evaluation of the Probable Modes of Failure.	19
B. Development of Interaction Relations for Bending in Two Planes	21
IV. ULTIMATE STRENGTH UNDER TORSIONAL MOMENT	26
A. Evaluation of the Probable Modes of Failure.	26
B. Development of Interaction Relations for Torsional and Vertical Moments	32
V. ULTIMATE STRENGTH UNDER COMBINED VERTICAL, LATERAL, AND TORSIONAL MOMENTS.	38
A. A Suitable Evaluation Procedure and Interaction Relations.	38
B. Application to a Tanker.	43
VI. CONCLUSION AND RECOMMENDATIONS	61
A. Analytical and Semi-Emperical Work	61
B. Experimental Program for Verification.	62
ACKNOWLEDGEMENT	64
REFERENCES.	65
APPENDIX I - CRITERIA FOR YIELD UNDER COMBINED STRESSES	68
APPENDIX II - THEOREMS OF LIMIT ANALYSIS.	71

NOMENCLATURE

- A = cross-sectional area of the plating and stiffeners for the hull girder section, and equal to $A_D + A_B + 2 A_S$
- A_B = cross-sectional area of the bottom including stiffeners
- A_D = cross-sectional area of the deck including stiffeners
- A_e = effective area of cross section of the hull girder accounting for buckling of plates under compression
- A_f = area of the flange for the symmetric section where $A_D = A_B = A_f$
- A_s = cross-sectional area of one side including stiffeners
- A_T = enclosed area of a hull girder midship section
- B = beam at the midship section
- b_e, b = effective width and actual width of plating, respectively
- C = a spring constant
- c = side to flange area ratio $\frac{A_s}{A_f}$ for the symmetric hull girder where $A_D = A_B = A_s$
- D = depth of the midship section
- D_{xy} = effective torsional rigidity for an orthotropic plate
- D_x, D_y = flexural rigidity of an orthotropic plate in the x and y directions, respectively
- E, E_t = elastic and tangent moduli of the material, respectively
- G = shear modulus of elasticity

NOMENCLATURE (CONT'D)

- g = the distance from the center of the deck area to the plastic neutral axis
- h_i = equivalent thickness of an orthotropic plate (with stiffeners diffused) in the i direction
- I_i = moment of inertia of the cross section of a structural member in the i direction
- I_{pc} = polar moment of inertia of a cross section with respect to an enforced axis of rotation
- k = St. Venant torsion constant for a section
- l = length, e.g., span of a stiffener
- M_{bp} = hull ultimate moment due to plate buckling failure
- M_i = initial yield moment defined by $(SM)_e \times \sigma_y$
- M_{max} = maximum hogging (or sagging) wave bending moment
- M_{min} = minimum sagging (or hogging) wave bending moment
- M_{xe} = effective plastic moment in the vertical direction, including the effect of buckling of plating between stiffeners on the fully plastic collapse moment
- M_x, M_y = bending moments in the vertical and lateral directions, respectively
- M_{x0}, M_{y0} = fully plastic collapse moments in the vertical and lateral directions, respectively
- m_x, m_y = non dimensional bending moments in the vertical and lateral directions defined as $\frac{M_x}{M_{x0}}$ and $\frac{M_y}{M_{y0}}$, respectively

NOMENCLATURE (CONT'D)

- N, N_0 = axial force and the fully plastic axial load for a section, respectively
- n = squash load ratio N/N_0
- r_c = radius of gyration of stiffener, including an effective area of plating
- r_e = effective radius of gyration for a stiffener
- S = vertical shear force
- SM_p, SM_e = the plastic section modulus and the elastic section modulus, respectively
- S_0 = fully plastic yield shear force for the section
- s = non-dimensional shear force in the vertical direction defined as $\frac{S}{S_0}$
- T, T_0 = torsional moment and the fully plastic torque for a section, respectively
- t = non-dimensional torque given by T/T_0
- t_D, t_B, t_S = equivalent deck, bottom and side thicknesses for an idealized hull girder; these include areas of stiffeners
- t_f = flange thickness including stiffener areas for the symmetric hull girder where $t_f = t_D = t_B$
- w = a curve parameter

NOMENCLATURE (CONT'D)

- α = aspect ratio of a plate
- ϕ = failure stress ratio defined as the ratio of the average failure stress to the yield stress in compression
- Φ = a stress function
- n = a plasticity factor = $\sqrt{\frac{E_t}{E}}$
- η_1, η_2 = distances of the points that separate the tensile and compressive plastic zones from an edge
- ν = Poisson's ratio of the material
- Γ = warping constant
- τ_c, τ_{ce} = critical shear stress, e denotes the elastic range
- τ_j = a shear stress
- σ = a direct stress
- σ_c, σ_{ce} = critical buckling stress where e denotes the elastic case
- σ_i = an equivalent stress intensity based on the Huber, Mises, and Henkey plasticity hypothesis
- σ_p = the porportional limit of the material
- σ_y = the material yield stress

I. INTRODUCTION

The determination of the collapse load, which defines the true ultimate strength of a ship's girder, has become a topic of increased interest to the ship research and design communities. One of the reasons behind this interest is that knowledge of the limiting conditions beyond which a hull girder will fail to perform its function will, undoubtedly, help in assessing more accurately the true margin of safety between the ultimate capacity of the hull and the maximum combined moment acting on the ship. Assessing the margins of safety more accurately will lead to a consistent measure of safety which can form a fair and a good basis for comparisons of ships of different sizes and types. It may also lead to changes in regulations and design requirements with the objective of achieving uniform safety standards among different ships.

Unfortunately, the state-of-the-art in determining the true ultimate strength of a ship girder is not at the point where drastic changes in design standards can be made, although some modifications and improvements are possible at the present time. The definition and evaluation of the different modes of failure, though they have been investigated in recent years, are not complete. Various definitions of the ultimate strength of a hull have been proposed, but the most acceptable one is the recommendation reported by Committee 10 in the proceedings of the Third International Ship Structures Congress, Vol. 2, 1967 [1]*, quoted as:

"This occurs when a structure is damaged so badly that it can no longer fulfill its function. The loss of function may be gradual as in the case of lengthening fatigue crack or spreading plasticity, or sudden, when failure occurs through plastic instability or through a propagation of a brittle crack. In all cases, the collapse load may be defined as the minimum load which will cause this loss of function."

Thus, besides instability (buckling), yielding, and spreading of plasticity, fracture may also be a significant mechanism of a hull girder failure under certain circumstances of repeated cyclic loads. Fracture includes brittle and fatigue failures which demand careful attention to material quality and the design of details (brackets, stiffener's connections, welding, etc.) both of which are outside the scope of this report. This study is concerned with the overall ductile failure of the hull as a girder in which yielding, spread of plasticity, buckling, and post-buckling strength are limiting factors. The hull is considered to be subjected to various combinations of extreme seaway loads including vertical, lateral, and torsional moments.

In this report, a literature survey was conducted at the beginning of the project on the methods recently developed to analyze the ultimate strength of hull girders along with general structural analyses methods suitable for prediction of ship's ultimate strength. One of the pioneering work in this area is due to Caldwell [2] in which a simplified analysis procedure was

*Numbers in brackets indicate references at end of report.

presented for calculating the ultimate load for a single-deck ship. His solution makes it necessary to define a structural instability factor to enable predicting the maximum strength of the box girder. Although this factor was not developed in that paper, it is the key requirement. Faulkner [3] suggested a design method for taking this buckling effect into consideration, basically through a reduction factor. Betts and Atwell [4] provided numerical solutions of several limiting bending moments of two Naval ships. In the report [5] of the ISSC meeting in Tokyo, the ultimate longitudinal strength of ships was thoroughly discussed. Attention was focused on available analytical techniques for predicting the load carrying capacity of a ship which was considered to act structurally as a stiffened box girder. Reference [6] provides several chapters concerning hull girder failure modes, margins of safety, and hull girder reliability. A ship structure committee report [7] presents a study of ship gross panels behavior and ultimate strength under combined loadings. Such gross panels constitute the basic structural elements in ships, and knowledge of their behavior and ultimate strengths is essential in determining the total hull girder ultimate strength. References [8] to [44] present some of the work which has been done in the ultimate strength of ships and provided some important information which will be referred to later in this report. Unfortunately, most of the work conducted in the past relates to the ultimate strength under vertical bending moment only (or the vertical collapse moment) with very little attention given to the fact that lateral and torsional moments are also present and may have an effect on the ultimate strength. Also, existing literature on model experiments and testing of box girders up to their ultimate strength is very limited [8,9,10,11,12].

From the literature survey, it was apparent that a clear distinction should be made between two types of failure (excluding fracture) of the hull girder under extreme loads:

- a. Failure due to spread of plastic deformation as can be predicted by the plastic limit analysis and the fully plastic moment.
- b. Failure due to instability and buckling of the gross panels making up the hull girder.

These two types of failure require separate methods of analyses as is the case in the usual elastic analysis where the possibility of buckling must be considered separately.

II. ULTIMATE STRENGTH UNDER VERTICAL MOMENT

One of the objectives of this section is to identify the possible modes of failure of the hull girder of a ship subjected to vertical bending moment only. The effects of the lateral and torsional moments will be discussed in the next sections. Another objective of this section is to evaluate, select, and modify existing methods for the determination of the hull ultimate strength and to critically examine their basic underlying assumptions in order to establish their validity range.

A. Identification of Possible Modes of Failure

As mentioned in the introduction, hull failure may assume one of several modes. Generally, it will not be known prior to conducting the failure analysis which mode of failure will be the governing one, i.e., which will give the smallest collapse vertical moment. A general procedure which provides a check of several modes of failure as parts of its components is, therefore, essential.

Under extreme vertical moment, it is expected that the hull girder strains will increase to a point where either the yield strength of the "column" or "grillage" is reached, or the "column" or "grillage" is buckled. In the former case, several methods may be used for predicting the ultimate strength. These include the initial yield moment, the fully plastic collapse moment, and the shakedown moment. On the other hand, if the "column" or "grillage" has a low critical buckling stress, other modes of failure will be governing and include flexural buckling or tripping of stiffeners and overall grillage failure.

Thus, excluding fatigue and brittle fracture, we may classify the possible modes of failure under:

1. Failure due to yielding and plastic flow.
 - The Plastic Collapse Moment
 - The Shakedown Moment
 - The Initial Yield Moment
2. Failure due to instability and buckling.
 - Failure of plating between stiffeners.
 - Panel failure mode (flexural buckling or tripping of longitudinals).
 - Overall grillage failure mode.

Each one of the above modes will be discussed separately in the following subsections.

B. Evaluation of Failure Due to Yielding and Plastic Flow

Several methods can be used in the evaluation of this failure mode. Each method is based on some assumptions and approximations which will be discussed and analyzed in the following paragraphs. Additional discussion of these methods can be found in reference [13].

1. The Plastic Collapse Moment

In this approach, it is postulated that the ultimate collapse condition is reached when the entire cross section of the hull including sides has reached the yield state. It is assumed that the material is elastic-perfectly-plastic and the loads do not change direction and increase proportionally up to the collapse loads. This means that the change in the bending moment direction (hogging/sagging) is not accounted for. It is further assumed that the compressed parts of the hull will remain effective, i.e., no buckling, and that the effects of axial forces and shear forces can be neglected.

With these simplifications, Caldwell [2] obtained an expression for the full plastic collapse moment " M_{x_0} " in the form,

$$M_{x_0} = (SM)_p \sigma_y \quad (1)$$

where

M_{x_0} = fully-plastic moment

σ_y = yield strength of the material

$(SM)_p$ = plastic section modulus given by

$$(SM)_p = A_D g + 2A_S \left(\frac{D}{2} - g + \frac{g^2}{D} \right) + A_B (D-g) \quad (2)$$

where

A_D = cross section area of the deck including stiffeners

A_B = area of the bottom including stiffeners

A_S = area of one hull side including stiffeners

D = depth of the midship section

g = distance from the center of the deck area to the plastic neutral axis given by

$$\frac{g}{D} = \frac{A_B + 2A_S - A_D}{4A_S} \quad (3)$$

In this report, Caldwell's concept is extended to include some of the factors neglected in deriving equations (1), (2), and (3). Attention is focused here on the effects of shear forces, axial forces, and buckling of plates between stiffeners which are subjected to compressive forces.

a. The Effect of Shear on the Fully Plastic Collapse Moment

Here, consideration is given to the fact that shear will be present and, depending on its magnitude, may have some effect on the fully plastic collapse load. In plating, where only direct and shear stresses " σ " and " τ " exist, the condition that the material does not violate the yield condition can be written as (see Appendix I):

$$\sigma^2 + \beta^2 \tau^2 \leq \sigma_y^2 \quad (4)$$

where

$$\begin{aligned} \beta &= \sqrt{3} \quad \text{for Von Mises condition} \\ &= 2 \quad \text{for Tresca condition} \end{aligned}$$

and the resulting bending moment (M_x) and shear force "S" in a box girder are given by:

$$\begin{aligned} M_x &= \int_A \sigma z \, dA \\ S &= \int_A \tau \, dA \end{aligned} \quad (5)$$

where A is the cross-sectional area of plating and stiffeners and z the distance to the neutral axis.

For any cross section, the yield curve for M and S are given by [14]:

$$\begin{aligned} M &= v \sigma_y \int_A \frac{z^2}{\sqrt{1 + v^2 z^2}} \, dA \\ S &= \frac{\sigma_y}{\beta} \int_A \frac{dA}{\sqrt{1 + v^2 z^2}} \end{aligned} \quad (6)$$

Equations (6) can be evaluated for a given cross section to furnish an interaction curve in the M, S plane in terms of the parameter v. For a symmetric box girder ($A_D = A_B = A_f$), an approximate interaction relation results:

$$s = \frac{S}{S_0} = \frac{\operatorname{sech} w + c w \operatorname{csch} w}{1 + c}$$

$$m = \frac{M}{M_{x_0}} = \frac{2 \tanh w + c(\operatorname{coth} w - w \operatorname{csch}^2 w)}{2 + c}$$
(7)

where

$$c = \frac{A_s}{A_f}$$

w = curve parameter

$A_f = A_D = A_B$ = flange area

Limiting cases:

- i. As $c \rightarrow 0$, i.e., for a very wide-flange box girder, the interaction curve reduces to:

$$s = \frac{1}{\cosh w}$$

$$m = \tanh w$$

or,

$$s^2 + m^2 = 1 \quad (\text{circle})$$
(8)

- ii. As $c \rightarrow \infty$, i.e., for a solid rectangular section or a narrow-flange box girder, the interaction relations are:

$$s = w \operatorname{csch} w$$

$$m = \operatorname{coth} w - w \operatorname{csch}^2 w$$
(9)

Figure 1 shows the interaction curves for $c = 0$ and $c = \infty$ which are fairly close to each other. The intermediate case of $c = 1$ is also plotted. In all cases, the fully plastic collapse moment (longitudinal) " M_{x_0} " and the fully plastic shear force S_0 for symmetric sections is given by:

$$M_{x_0} = \frac{\sigma_y D}{2} A_f (2 + c)$$
(10)

$$S_0 = \frac{2 \sigma_y}{\beta} A_s$$
(11)

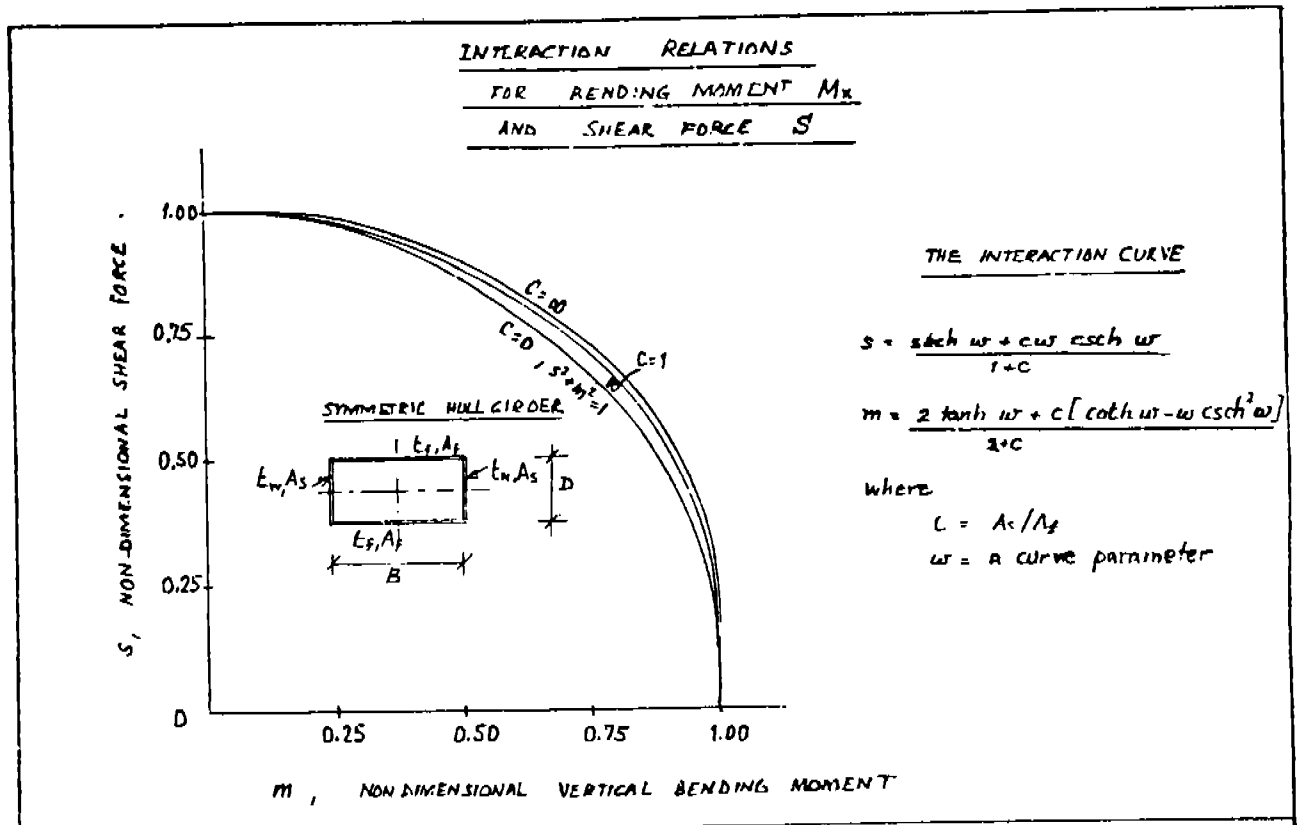


FIGURE 1. Interaction Curves Under Bending Moment M_x and Shear Force S

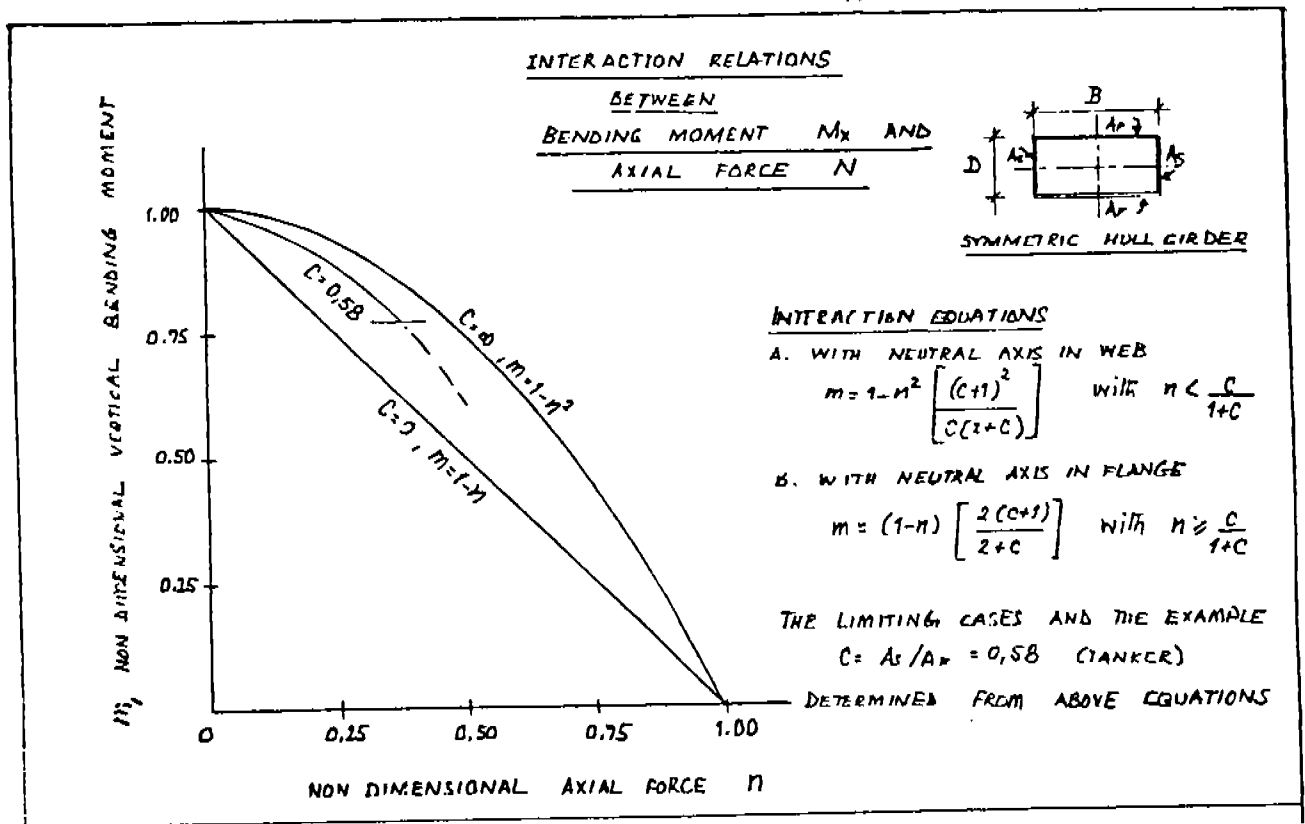


FIGURE 2. Interaction Curves Under Bending Moment M_x and Axial Force N

Any point on the interaction curve corresponds to a fully plastic section of the hull girder. Points inside the curve represent stress distributions which are less than fully plastic. Points outside the curve correspond to moment and shear force magnitudes for which no stress distribution can be found that will not exceed the yield.

By entering the appropriate "c" curve in Figure 1 with the value of,

$$s = \frac{S}{S_0}$$

the reduction in the fully plastic moment due to the presence of shear can be estimated. This effect will be examined for actual ships in Section V of this report.

b. The Effect of the Axial Force on the Fully Plastic Collapse Moment

Although the axial forces in a typical ship hull are very small, their effects on the fully plastic moment will be examined briefly here. As the axial load increases, the neutral axis of the hull may shift depending on the geometry of the section and the manner in which the load is increased. However, attention is focused here at the fully plastic stress distribution and the variation in the neutral axis position prior to the fully plastic state is not important.

The stress resultants in the fully plastic state are:

$$M_x = \int_A \sigma z dA \quad ; \quad N = \int_A \sigma dA \quad (12)$$

and, for a symmetric hull girder, the interaction relation was derived as:*

$$m = 1 - n^2 \frac{(c+1)^2}{c(2+c)} \quad (13)$$

where

$$m = \frac{M}{M_{x_0}} \quad ; \quad n = \frac{N}{N_0} \quad ; \quad c = \frac{A_s}{A_f}$$

$$N_0 = 2 \sigma_y A_f (1+c) = \text{fully plastic axial load}$$

N is the acting axial load and M_{x_0} is defined by equation (10).

Figure 2 shows the interaction relations for the limiting cases when $c = 0$ and $c = \infty$, which correspond to $m = 1-n$ and $m = 1-n^2$, respectively. The spread between the curves here is larger than in the shear interaction curves. A more accurate estimate of "c" was therefore necessary for an additional curve to be plotted. For a 200,000 ton displacement tanker (see application in Section V) the value of "c" was calculated to be 0.58 and the corresponding interaction curve is plotted in Figure 2.

*Equation (13) assumes that the final neutral axis lies in the webs.

c. The Effect of Buckling of Plates Between Stiffeners on the Fully Plastic Collapse Moment

Plates between stiffeners in the compressed parts of the hull may buckle before the stress reaches the yield stress. In this case, only the effective area of the compressed parts of the hull must be used in calculating the plastic collapse moment. The term "effective" plastic collapse moment will be used here to indicate that if buckling occurs of plates between stiffeners, the "effective" plastic section modulus is less than the "fully" plastic section modulus given by Equation (2). Neglecting the effect of the axial force, the location of the neutral axis can be determined from the static equilibrium requirement:

$$\int_{A_e} \sigma_y d A_e = 0 \quad (14)$$

where A_e and $d A_e$ represent the "effective" area and an element of the effective area, respectively.

The effective plastic moment " M_{x_e} " is then calculated from:

$$M_{x_e} = \int_{A_e} \sigma_y z d A_e \quad \text{or} \quad M_{x_e} = \sigma_y \sum_i (\Delta A_e)_i d_i \quad (15)$$

where $(\Delta A_e)_i$ = small element of the effective area on the cross section

d_i = distance from the final neutral axis to the centroid of $(\Delta A_e)_i$.

References such as [15,16,17,18] may be used to determine the effective area for plating after buckling. Use of a digital computer is recommended for the determination of the neutral axis location from Equation (14) and the effective plastic moment " M_{x_e} " from (15).

2. The Shakedown Moment

Consideration is given in this method to the fact that the bending moment acting on the hull alternates between hogging and sagging. Because of the moment direction change, collapse may occur due to incremental plastic displacement or alternating plasticity [44]. Under the former type, a net plastic displacement takes place until an ultimate state (unserviceable hull) is reached where displacement increases without limit. Under the latter type of collapse, plastic displacement takes place and alternates between certain values. Such alternating plastic flow is damaging to the hull and has an effect similar to the elastic concept of fatigue, but the number of cycles involved is of a much lower order of magnitude (tens of cycles instead of millions of cycles). Since the hull can absorb only a finite amount of plastic energy, a safe hull shakes down to purely elastic behavior after a limited amount of plastic flow.

To prevent alternating plasticity, the following condition must be satisfied:

$$M_{\max} - M_{\min} \leq 2M_i = 2 \frac{M_{X_0}}{\alpha} \quad (16)$$

To prevent incremental collapse, the requirement is represented by the inequalities:

$$M_s + M_{\max} \leq M_{X_0} \quad (17)$$

$$M_s + M_{\min} \geq M_{X_0}$$

where M_s is the stillwater bending moment, M_{\max} is the maximum hogging (or sagging) wave bending moment, M_{\min} is the minimum sagging (or hogging) wave bending moment, M_{X_0} is the fully plastic collapse moment defined by Equation (1), M_i is the initial yield moment defined by Equation (19) and α is a shape factor defined as:

$$\alpha = \frac{M_{X_0}}{M_i} \quad (18)$$

It is evident from Equation (16) that if the moments vary between equal positive and negative values then maximum bending moment must be less than or equal to the initial yield moment " M_i ". This, in essence, places some importance on " M_i " as a lower bound estimate of hull strength for this particular mode of failure (yielding and plastic flow).

It should be noted that in shakedown analysis, the probability of occurrence of several bending moments which cause plastic flow in the hull over its lifetime is important. If such probability is high, then shakedown estimates of the hull strength can be important. Under these circumstances, however, if the moments vary between approximately equal positive and negative values, then the simple initial yield moment " M_i " is recommended for obtaining a low-bound estimate of the hull strength for this mode of failure, i.e., assuming premature buckling will not occur. If these conditions are not satisfied then the applicability of each formulation described above should be examined by evaluating the relevance of its underlying assumptions for the particular hull under consideration.

3. The Initial Yield Moment

In this simple method, it is assumed that the ultimate strength of the hull is reached when the deck (only) has yielded. The neutral axis position is assumed to be unchanged and the elastic section modulus to be governing. Premature buckling is assumed not to occur or to be dealt with separately as will be discussed in subsection "C" of this section. Using these simplifications, the initial yield moment is written as:

$$M_i = (SM)_e \sigma_y \quad (19)$$

where $(SM)_e$ is the elastic section modulus and σ_y is the tensile yield strength of the material.

The simplicity of this formulation and the fact that the elastic section modulus is usually calculated in the standard routine longitudinal strength calculations make it easy for use in design. Also, under certain circumstances (see subsection 2 above), the initial yield moment represents the maximum allowable moment as determined from shakedown analyses. It should be noted, however, that after evaluating the buckling modes of failure, the initial yield moment may turn out to be optimistic for some hull designs.

C. Evaluation of Failure Due to Instability and Buckling

Several buckling modes of failure may take place within hull grillages [7,13] and the adequacy of existing methods of predicting the ultimate collapse load of the hull depends on the particular mode of grillage failure. Some experience has been gained in certain modes of grillage failure and correspondingly some expressions have evolved. In some other modes of failure, however, the progress has been slow and either no well-established reliable design procedure is available, or in some cases, no clear measure of the relative reliability between the available procedures can be affirmed [7].

Some individual failure modes are discussed below. The two major modes of grillage failure which are likely to lead to hull ultimate collapse condition are the panel buckling mode (which includes column flexural buckling and column tripping) and the overall grillage failure mode. Failure of plates between stiffeners can be considered as local failure, particularly for longitudinally stiffened ships, but some considerations are given to it because once buckling of the plates occurs, a reduction in the strength of the column (plate-stiffener combination) takes place due to the reduction in plate effectiveness.

1. Failure of Plating Between Stiffeners [13]

This mode of failure can be important in transversely framed ships, especially in deck plating near hatch openings. Unlike columns, it is well known that plates can carry loads beyond their critical buckling loads provided that the slenderness ratio of the plate is large. The ultimate compressive load can be determined in this case using von Kármán's concept which states that the load-carrying capacity of the plate is exhausted when the edge stress approaches the yield point. Under these conditions, the hull ultimate moment due to plate buckling failure " M_{bp} " can be written as:

$$M_{bp} = (SM)_e \times \phi \times \sigma_{yc} \quad (20)$$

where

$(SM)_e$ = elastic section modulus

σ_{yc} = compressive yield strength of the material

ϕ = failure stress ratio = $\frac{\text{average failure stress}}{\text{yield stress } \sigma_{yc}}$

ϕ depends on the effectiveness of the plating after buckling and can be written also as:

$$\phi = \frac{b_e}{b} \quad (21)$$

where b_e is effective width and b is the actual width.

According to von Kármán, the effectiveness of the plate at failure (when edge stress is equal to yield stress) is given by:

$$\begin{aligned} \frac{b_e}{b} &= \frac{\pi}{\sqrt{3(1-\nu^2)}} \frac{t}{b} \sqrt{\frac{E}{\sigma_{yc}}} \\ &= \frac{1.9}{\beta} \quad \text{for steel} \end{aligned} \quad (22)$$

where $\beta = \frac{b}{t} \sqrt{\frac{\sigma_{yc}}{E}}$

E = modulus of elasticity

ν = Poisson's ratio

A better agreement with experiments can be obtained by using in (22) instead of the constant factor,

$$\frac{\pi}{\sqrt{3(1-\nu^2)}} = 1.9$$

a factor "k" varying with the non-dimensional parameter $1/\beta$. Timoshenko, in Reference [16], gives the experimental values of the factor k which decreases slightly with increasing values of $1/\beta$.

For wide ship plating subject to uniaxial compression only, analytical values of the effective width b_e can be obtained from curves present in [19]. Under biaxial as well as uniaxial loading conditions, the effective width " b_e " at failure can be determined from design curves presented in [14] using an iterative procedure.

In Reference [17], Faulkner proposed a semi-empirical formula for the effective width to be used instead of Equation (22). Based on investigating several effective width formulas, he suggested for ship use an effective width at failure given by:

$$\frac{b_e}{b} = \frac{2}{\beta} - \frac{1}{\beta^2} \quad (23)$$

Figure 3 shows a comparison of the effective width according to von Kármán, Timoshenko and Faulkner suggested formulations.

A modification of the effective width is suggested in Reference [20] for the inclusion of residual stresses using a reduction factor. The effect of initial deflection on the effective width can be approximately incorporated using References [18,19].

2. Panel Buckling Mode of Failure

In this failure mode, collapse occurs by column-like buckling of the longitudinal stiffeners with their effective platings between the transverse frames. In most cases, because of the direction of the usual lateral loads on bottom and deck gross panels, buckling occurs such that stiffeners flanges are under tension. But buckling may also occur in the opposite direction and in this case, because most of the stiffener is under compression, lateral torsional buckling (tripping) of the stiffeners may take place (see Reference [21]). For this reason, two separate analyses are necessary as follows:

a. Flexural Buckling of Stiffeners

Here, the hull ultimate strength is considered to be governed by the ultimate load-carrying capacity of the longitudinal stiffeners (together with the effective plating) between the transverse frames; and buckling is assumed to be purely flexural. Elasto-plastic finite-element programs [21,22] can be useful in the prediction of the stiffeners ultimate loads. Grillage representation and beam-column elasto-plastic behavior such as adopted by Kondo [23] can be also used. Development of parametric studies, design charts, and simplified design formulas based on these approaches is very desirable for the usual routine design work.

The hull ultimate moment due to panel buckling failure " M_{bn} " may be written in the form:

$$M_{bn} = (SM)_e \times \phi \times \sigma_{yc} \quad (24)$$

where ϕ is the average failure stress ratio (taken into consideration plate effectiveness).

For the simply supported case of straight columns, Euler critical stress is considered to be close to the failure stress if buckling occurs in the elastic range.

$$\sigma_c = \frac{\pi^2 E r_c^2}{l^2} \quad ; \quad r_c = \frac{I}{A} \quad (25)$$

The radius of gyration r_c in (25) depends on the effective width of plating working with the stiffener. The effective width in turn depends on the magnitude of the stress and should be taken at stress equal to the failure stress σ_c ; and therefore an iterative procedure is necessary.

ULTIMATE BUCKLING
STRENGTH OF UNSTIFFENED
THIN PLATES

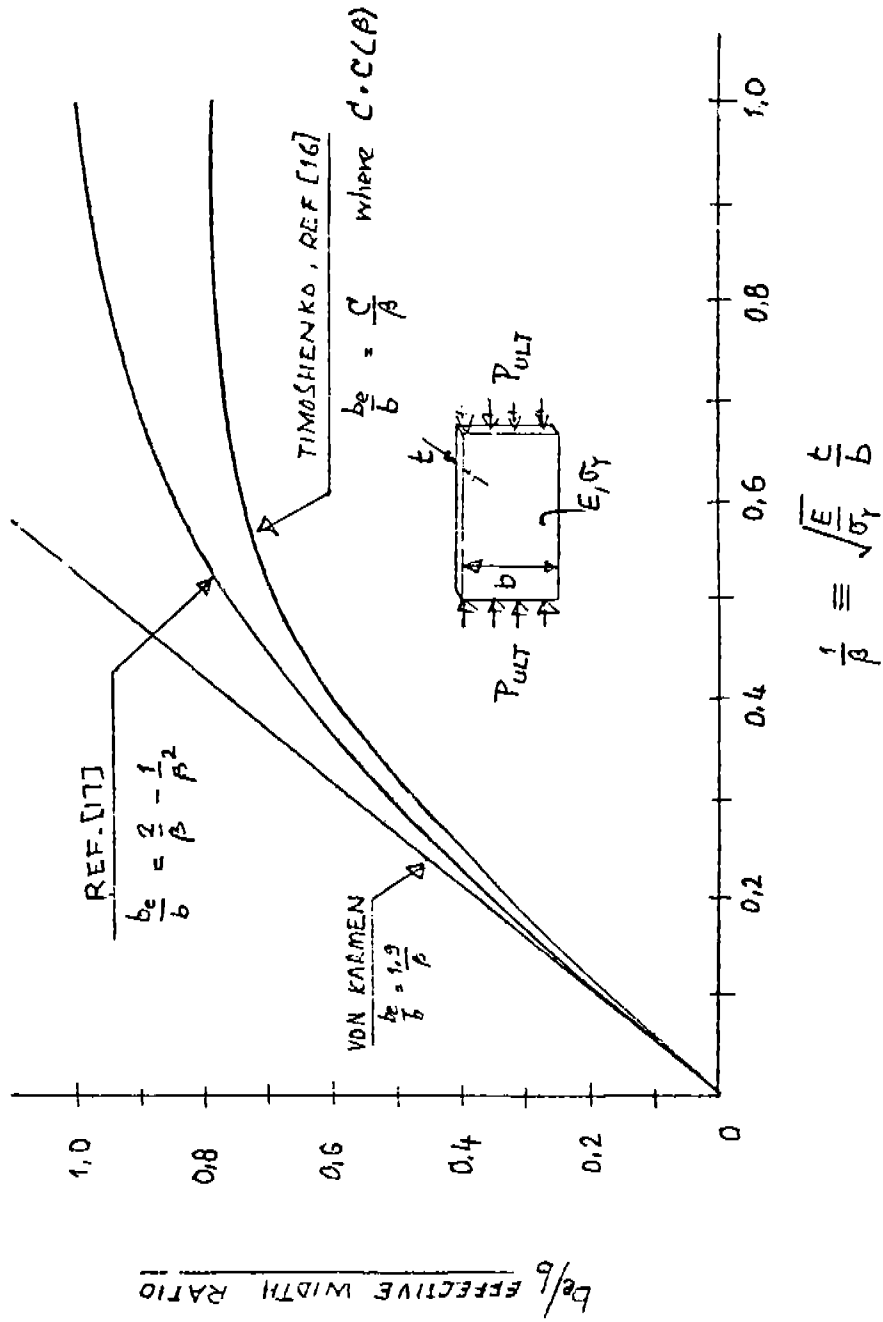


FIGURE 3. Effective Breadth of Plates

Equation (25) cannot be used when the resulting σ_c is greater than the proportional limit stress of the material. Between the proportional limit and the yield point, the tangent modulus E_t instead of E may be used in (25). The tangent modulus " E_t " is to be determined from a compression test diagram with an iterative procedure necessary to obtain E_t at σ_c . In the absence of a compression test diagram, Bleich [24] formulation using a quadratic parabola may be used:

$$E_t = E \frac{(\sigma_{yc} - \sigma) \sigma}{(\sigma_{yc} - \sigma_p) \sigma_p} \quad (26)$$

where σ_p is the proportional limit of the material.

A limiting case is when the compressive stresses reach the yield point of the material " σ_y ", in which case, the buckling strength can be taken as the yield strength of σ_{yc} the material.

In Reference [20], a suggestion is made for the inclusion of the effect of residual stress by subtracting it from the proportional limit on the basis of experiments conducted at Lehigh University.

b. Lateral-Torsional Buckling of Stiffeners (Tripping)

This mode of failure is a result of coupled flexural and torsional modes of buckling. Some elastic buckling expressions were obtained by Bleich [24], but no satisfactory general method exists for the inelastic tripping of stiffeners welded to plates and for the prediction of the inelastic collapse strength. Bleich's approximate formulation results [24]:

$$\sigma_c = \frac{\pi^2 E}{(\ell/r_e)^2} \quad (27)$$

where ℓ is the stiffeners length and r_e is the effective radius of gyration. The effective radius of gyration for a variety of stiffener shapes and for stiffeners which can rotate with or without restraint around the enforced axis of rotation (intersection line with the plate) can be obtained from curves and expressions given in Reference [24]. Other formulations such as discussed in [21,25] using folded-plate analysis can be used to estimate the tripping critical load.

For the case of a symmetrical stiffener with an enforced axis of rotation taken as the intersection line with the plate, Bleich [24] obtained the following expression for " r_e " to be used in (27):

$$r_e^2 = \frac{\ell^2}{\pi^2 E I_{pc}} \left[GK + 2 \sqrt{E(\Gamma + a^2 I_y)C} \right] \quad (28)$$

where l is the length, I_{pc} is the polar moment of inertia of the cross section with reference to the enforced center of rotation, G is the shear modulus of elasticity, r is the warping constant, I_y is the moment of inertia about the axis of symmetry, C is the rotational spring constant at the intersection line of the stiffener with the plate, and K is the St. Venant torsion constant of the section.

It should be noted that, in some cases, local web buckling of stiffener before torsional failure is possible. For these cases, Bleich [24] gives a solution for a T stiffener with the web regarded as a plate hinged on one edge and elastically restrained by the flange on the other.

The hull ultimate bending moment due to stiffeners tripping mode of failure can be determined from Equation (24) provided that the appropriate value of the tripping collapse stress and, therefore, the value of ϕ can be accurately determined. It may be noted, however, that if tripping brackets are present and are properly design and spaced, this failure mode will not be a governing factor in the overall ultimate strength of the hull.

3. Overall Grillage Failure Mode

This collapse mode involves the overall buckling of the entire grillage including the longitudinal as well as the transverse stiffeners. The hull ultimate moment due to overall grillage failure can be estimated from:

$$M_{bg} = (SM)_e \times \phi \times \sigma_{yc} \quad (29)$$

where ϕ is the ratio of the average failure stress to the yield strength " σ_{yc} ".

For uniform grillages, the buckling loads and modes can be estimated from orthotropic plate formulas [26,27,28]. Under biaxial load, some interaction relations were developed in [7] showing the combination of critical loads for various aspect ratios and rigidities of both plates and stiffeners.

For grillages under uniaxial compression, the elastic buckling stress can be written in the form [26]:

$$\sigma_c = k \frac{\pi^2 \sqrt{D_x D_y}}{h_x B^2} \quad (30)$$

where D_x and D_y are the grillage flexural rigidities in the x- and y-directions; B is the length of the loaded edge; h_x is the equivalent thickness of the plate; and stiffeners " k " is a constant which depends on the boundary conditions as can be determined from [7].

In slender grillages, for which the elastic buckling stress is well below the yield point, a significant post buckling reserve may exist [19]. The ultimate strength in this case may be estimated from design charts presented in [15] from which the effective width at failure can be determined in an iterative manner. The effective widths are given in these charts for a

variety of biaxial loading conditions together with lateral pressure. The charts indicate, however, that the ultimate strength is little affected by the magnitude of the lateral load, particularly if the edge loads are larger than the critical buckling loads. This observation is in agreement with experimental results given in [21]. Also, according to these charts, an inplane load in the transverse direction has a small effect on the effective width if the inplane load in the longitudinal direction is much larger than the critical load. No experimental confirmation, however, exists for this latter observation.

The ultimate strength of the grillage and, therefore, the value ϕ can be predicted also using expressions given in [20]. In this case,

$$\phi = \frac{\sigma_c}{\sigma_{yc}} \left[\frac{\gamma + b_e/b}{\gamma + 1} \right] \quad (31)$$

where " σ_c " for wide and long grillages with sides elastically constrained are given in Reference [20], b_e/b is the plate effectiveness as given in subsection 1 above and γ is the area ratio of stiffener to plate. In this method [20], no allowance was made, however, to the non-linear large deformations which make the method suitable only for applications to grillages with heavy stiffeners.

The effect of the initial deflection on the ultimate collapse load for this mode of failure can be estimated from Reference [15] which presents design curves showing the effect of initial deflection on the effective width for a variety of inplane loads, lateral loads, stiffeners characteristics, and aspect ratios. The effect of the residual stresses can be approximately included using the formulation given in [20].

III. ULTIMATE STRENGTH UNDER LATERAL MOMENT

Lateral bending moments acting in a ship hull girder, unlike the vertical bending moment, are purely a wave-generated phenomenon. Model tests [29] indicate that, in magnitude, these loads may approach or exceed the vertical component, depending on wave obliqueness and the effective wave length. Sea trials on the Ocean Vulcan [30] show evidence that the maximum moment occurs at a wave to course angle of about 110° to 140° and that this component was frequently in phase with the vertical bending moment. This chapter is divided into two parts. First, the modes of failure under a pure lateral bending moment are considered. Following this, we investigate the interaction of bending moments acting in the vertical and horizontal planes simultaneously. By itself, the lateral bending moment would not be a governing factor in failure since the elastic and plastic section moduli associated with it are much greater than those associated with the vertical moment; whereas the load itself is about the same order of magnitude and possibly less in smaller vessels. The critical stresses associated with buckling instability are also likely to be larger because the sides' scantlings are usually heavier in order to allow for the hydrostatic pressure. Therefore, in the "B" section of this chapter we will consider the more important aspect which is the interaction with the vertical moment.

A. Evaluation of the Probable Modes of Failure

The first mode of failure considered here is the fully plastic yield of the hull considered as a box-beam. Then failure by the instability of the structural components is dealt with.

1. The Fully Plastic Collapse Moment

The evaluation of strength under a lateral bending moment may be done in a manner analogous to the estimation of the fully plastic collapse strength under a vertical bending moment dealt with in the last section. The plastic neutral axis, assuming that all the structural components remain stable through the entire range of load application, is located on the center line. It may then be shown that the fully plastic yield moment is given by:

$$M_{y0} = \sigma_y \left[A_s B + \frac{B}{4} (A_D + A_B) \right] \quad (32)$$

where A_s , A_D , and A_B are the areas at the side, deck, and bottom, respectively; σ_y is the material yield stress; and B , the beam of the vessel. If the section is symmetric with respect to both the vertical and horizontal planes, Equation (32) reduces, with $A_D = A_B = A_f$ to:

$$M_{y0} = \sigma_y A_s B \left(1 + \frac{1}{2c} \right) \quad (33)$$

where c is the ratio A_s/A_f . As noted before, failure under the lateral bending moment alone is unlikely to be a governing mode in the failure of the hull.

2. Failure by Structural Instability

We may again consider instability in the usual hierarchical sequence: that of plating between stiffeners, of the column formed by the stiffener and an effective breadth of plating; and of the stiffened plate panel. The investigation may pertain either to the side or to the deck. The methods of analysis have already been outlined in Section II dealing with ultimate strength under a vertical bending moment and only a brief discussion is given here. Once the compressive mode of failure is identified, the ultimate strength is given by:

$$M_n = (SM)_e \times \phi \times \sigma_{yp} \quad (34)$$

where ϕ is the average failure stress/material yield stress ratio.

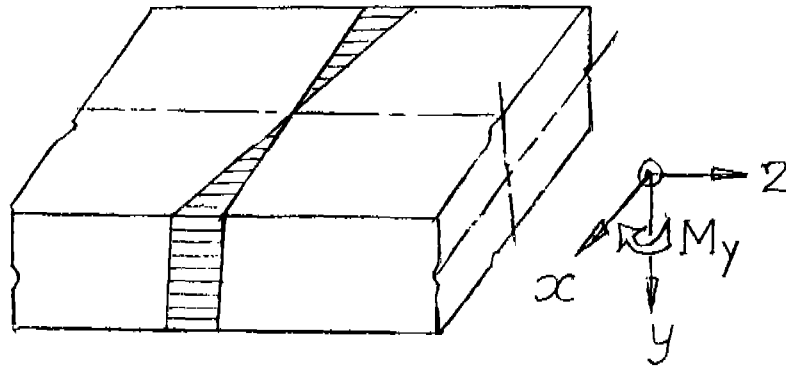


FIGURE 4. Stress Distribution - Lateral Bending Moment

One may note here that under the lateral bending moment the bottom and the deck are subjected to bending in their own plane (see Figure 4 above). The critical stress in the case of unstiffened plates under a non-uniform longitudinal compression may be given as:

$$\frac{\sigma_c}{\sqrt{\tau}} = k \frac{\pi^2 E}{12(1-\nu^2)} \left(\frac{t}{b}\right)^2 \quad (35)$$

where τ is the ratio E_t/E , taken as unity in the elastic range. In the inelastic range, one may obtain $\sigma_c/\sqrt{\tau}$ and then c using the Ostenfeld-Bleich parabola for E_t/E . Plate factors k for various possible stress distributions may be found in Reference [24, pp. 401 and 410], for the simply supported case. Plate factors for the case of the deck under inplane bending are, in general, higher than the case where the deck is under uniform compression. For instance, under the stress distribution shown in Figure 5, with $\sigma_2/\sigma_1 = -1$ and $\alpha = a/b$,

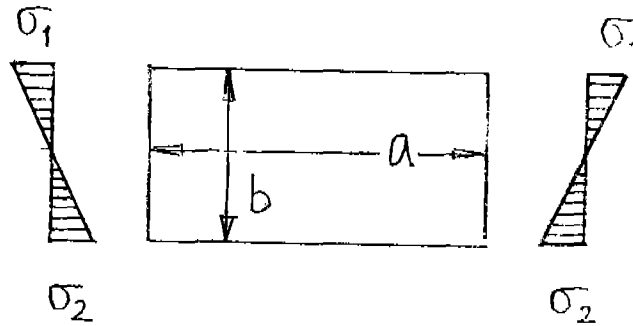


FIGURE 5. Inplane Bending Stress

we have,

$$\begin{aligned}
 k &= 24 \quad ; \quad \alpha \geq 2/3 \\
 &= 24 + 73(2/3 - \alpha)^2 \quad ; \quad \alpha < 2/3
 \end{aligned}
 \tag{36}$$

compared to $k = 4.0$ in the uniform compression case for a simply supported plate. For the case where the plate is stiffened by a longitudinal stiffener, and is subjected to pure bending in its plane, Bleich [24, p. 422] presents results for the plate factor as a function of the aspect ratio and the factor:

$$\gamma = \frac{EI}{bD}$$

i.e., the stiffener/plate rigidity ratio. The plate factors, in general, are seen to be much higher than those for the uniform compression case.

B. Development of Interaction Relations for Bending in Two Planes

Based on the last section analysis, it is concluded that the lateral bending alone is not a governing factor in failure. We now consider the interaction of the vertical bending moment with the lateral moment. Again, the cases considered are that of the fully plastic yield moment and failure under compressive instability.

1. Hull Box Girder Under Bending in Two Planes - Plastic Moments Interaction

Consider the hull girder subjected to a vertical bending moment M_x acting simultaneously with the lateral bending moment M_y . The non-dimensional bending moment ratios in this case are:

$$\begin{aligned}
 m_x &= \frac{M_x}{M_{x0}} \quad \text{and,} \\
 m_y &= \frac{M_y}{M_{y0}}
 \end{aligned}
 \tag{37}$$

where M_{x_0} and M_{y_0} are the fully plastic yield moments of the girder in the two planes, as given by Equations (1) and (32), respectively. For this load case, assuming that the section remains stable throughout the entire load range, two types of yield geometry are possible as shown in Figure 6.

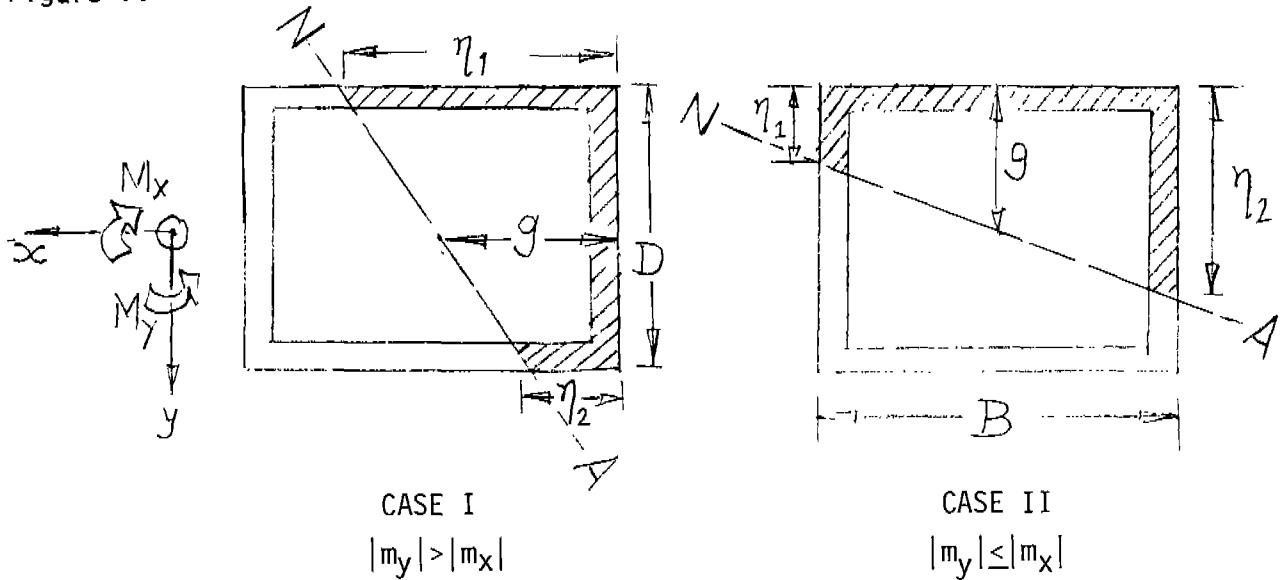


FIGURE 6. Full Yield Geometry Under Vertical and Lateral Moments

The two cases differ in the position of the neutral axis that separates the section into tensile and compressive zones. η_1 and η_2 are the distances of the points that separate these zones from an edge (side or deck, as the case may be) as shown. In a given girder, either stress distribution may occur depending on the relative magnitudes of m_x and m_y . For the ship hull considered as a box-beam, we limit our analysis to Case II where $|m_y| \leq |m_x|$. It is possible to derive the interaction relationship in either case; but the case where $|m_y| > |m_x|$ is thought not to be a typical situation for a ship. For the yield geometry shown in Case II, the following equations were derived:

$$M_x = \sigma_y [A_D g + A_B(D-g) + A_s \frac{\eta_1}{D} (2g-\eta_1) + 2A_s(\frac{D}{2} - g) + A_s \frac{\eta_2}{D} (2g-\eta_2)] \quad (38)$$

Note that (38) reduces to Equations (1,2) for the case where M_x acts alone. In general:

$$\frac{g}{D} = \frac{\eta_1 + \eta_2}{2D} \quad (39)$$

The lateral moment is derived as:

$$M_y = \sigma_y A_s \frac{B}{D} (\eta_2 - \eta_1) \quad (40)$$

If M_x acts alone, $\eta_1 = \eta_2 = g$ and $M_y = 0$. From the requirement that the net axial force on the section is zero, we have:

$$A_B - A_D + 2A_S \left(1 - \frac{\eta_1}{D} - \frac{\eta_2}{D}\right) = 0 \quad (41)$$

This reduces to Equation (3) for the case where M_x acts alone. On eliminating η_1 and η_2 from Equations (38) to (41), one obtains the interaction relationship for m_x and m_y . This is given by:

$$m_x + k m_y^2 = 1 \quad , \quad |m_y| \leq |m_x| \quad (42)$$

where,

$$k = \frac{(A + 2 A_S)^2}{16 A_S (A - A_S) - 4(A_D - A_B)^2} \quad (43)$$

$$A = A_D + A_B + 2 A_S$$

In Equations (42) and (43), m_x and m_y are the non-dimensional bending moments defined by Equation (37). The fully plastic bending moments M_{x_0} and M_{y_0} are given by Equations (1) and (32), respectively. The value of g for evaluating M_{x_0} is given by Equation (3).

For the case of a symmetric girder where $A_D = A_B = A_f$, we may simplify Equation (43) with $c = A_S/A_f$ to:

$$k = \frac{(1 + 1/2c)^2}{(1 + 2/c)} \quad (44)$$

The fully plastic yield moments in this case are given by:

$$M_{x_0} = \sigma_y A_f D \left(1 + \frac{c}{2}\right) \quad (45)$$

$$M_{y_0} = \sigma_y A_S B \left(1 + \frac{1}{2c}\right)$$

and the interaction relation is given by Equation (42). For the particular case of the uniform box beam, i.e., $A_S = A_D = A_B$, we have

$$k = 3/4$$

The interaction relations for some representative values of k are shown in Figure 7.

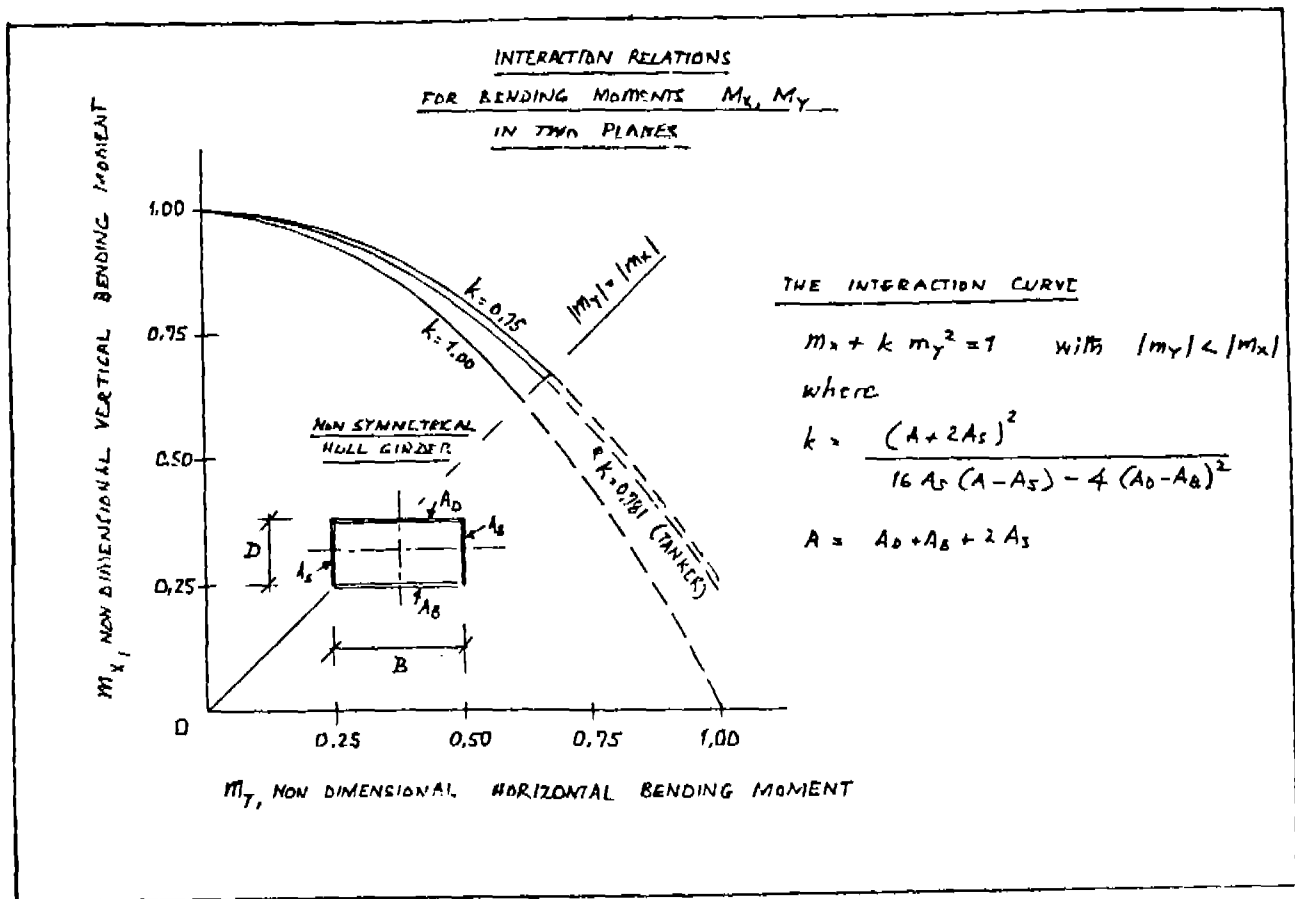


FIGURE 7. Interaction Curves Under Vertical and Lateral Moments.

2. Instability and Buckling Under Non-Uniform Edge Compression

Consider compression failure of the girder under the simultaneous action of the bending moment in the vertical and horizontal planes. The effect of this loading is to introduce, as a general case, non-uniform uniaxial edge compression in the sides and the flanges. Methods of analysis have already been indicated for this loading condition in subsection A-2 of this chapter.

IV. ULTIMATE STRENGTH UNDER TORSIONAL MOMENT

A combination of factors, such as oblique seas, unsymmetrical structural and cargo weights or motion induced angular accelerations, may cause the ship structure to be subjected to torsion. The response of the hull girder to this torque is characterized primarily by twisting of the structure about some longitudinal axis. This produces shear stresses in the plane of the torque. This also gives rise to diagonal tensile and compressive stresses that may induce plate buckling or give rise to stress concentrations at structural discontinuities. The primary shear stresses are usually negligible in tankers and similar closed-deck type ships. However, both the shear and the consequent direct stresses may be significant in the case of ships with large deck openings, container ships being an obvious example. Special consideration to torsional loading would also be necessary in the case of other hull forms such as catamarans. Heavy-lift ships are another case in question where torsional effects may have to be investigated. In general, any service condition that may increase torsional loads or any structural configuration that reduces torsional rigidity is obviously suspect. In this connection, one may note that transverse bulkheads do not contribute to torsional strength as they do to racking.

It may be appropriate here to mention briefly how one may estimate the torsion loads and the response of a ship hull girder to those loads. The wave torque applied to the ship by an oblique sea is computed by a quasi-static procedure similar to the usual longitudinal strength calculations. The resulting load is combined with any stillwater torque arising from a non-symmetrical weight distribution or any dynamic effects arising from angular accelerations. For a discussion of the procedure, one may refer to [31] and [32]. Usually one neglects the torque arising from horizontal pressure components; but as pointed out in [32], this would grossly underestimate the torque in the case of open-deck ships where the shear center is nearer to the bottom. Empirical formulae for estimating the vertical torsional moment may also be found in [31] and [32].

The response of a closed-deck hull girder to the applied torsional moment is usually computed assuming that the resulting shear stresses are uniform across the thickness of the plating and that the product of shear stress and thickness (the shear flow) is constant around the closed cell. Shear stresses are determined for this case using the well-known Bredt expression. An extension of this method is applied to the case of the statically indeterminate closed multi-cell structure [31].

This section is divided into two parts, the first of which evaluates the probable modes of failure under pure torsional moments. The determination of strength under those modes is also indicated. The second part is concerned primarily with the interaction between the torsional moment and a vertical bending moment acting simultaneously.

A. Evaluation of the Probable Modes of Failure

We now consider the failure of a hull girder subjected to a pure torsional moment. The girder may fail either by a fully plastic yielding of the entire cross section or by compressive failure of the components of the beam cross section. In the former case, the entire cross section is assumed stable. The

postulated failure mechanisms are of course simplified in that these two modes are considered separately. The possibility of interaction is readily conceded, but not explicitly accounted for in the analysis.

1. Pure Plastic Torsion of Hull Girders

Consider first the case of a beam loaded in one plane, z being the beam axis. The beam will yield only when it is plastic across the entire cross section. With the notation that τ_{ij} is the shear stress parallel to the i and perpendicular to the j direction, yield occurs when:

$$\tau_{xz}^2 + \tau_{yz}^2 = \left(\frac{\sigma_y}{\beta}\right)^2 \quad (46)$$

The equilibrium condition to be satisfied by the stress components is given by:

$$\frac{\partial \tau_{xz}}{\partial x} + \frac{\partial \tau_{yz}}{\partial y} = 0$$

If we introduce a stress function ϕ such that,

$$\tau_{xz} = \frac{\partial \phi}{\partial y} \quad \text{and} \quad \tau_{yz} = -\frac{\partial \phi}{\partial x}$$

we see that the equilibrium equation is identically satisfied. The yield condition requires that the gradient of ϕ is a constant of magnitude σ_y/β . Generally speaking, ϕ must be a constant on each boundary of a multiply connected region, e.g., a tube. In the case of a simply connected cross section, the boundary conditions may be satisfied by taking $\phi = 0$ on the boundary.

The maximum plastic torque the solid cross section can sustain is then given by [14]:

$$T_0 = \int_A (x \tau_{yz} - y \tau_{xz}) dA = 2 \int_A \phi D dA \quad (47)$$

For an annular cross section, the limits of integration may be altered appropriately. For example, the stress function for the first octant of a solid square of side $2D$ is:

$$\phi = \frac{\sigma_y}{\beta} (D-x)$$

and the total maximum plastic torque for that square is:

$$T_0 = \frac{8}{3} \frac{\sigma_y}{\beta} D^3 \quad (48)$$

For a hollow square with outer dimension $2D_o$ and inner dimension $2D_i$, the maximum plastic torque is:

$$T_o = \frac{8}{3} \frac{\sigma_y}{\beta} (D_o^3 - D_i^3) \quad (49)$$

Hence, for a uniformly thin-walled square box girder, and considering only the first-order terms in the thickness "t", we have:

$$T_o = 8 \frac{\sigma_y}{\beta} D_o^2 t \quad (50)$$

For the general case of a thin-walled box girder, if t is the minimum thickness of the section, then the fully plastic torque is given by:

$$T_o = 2t \frac{\sigma_y}{\beta} A_T \quad (51)$$

where A_T is the enclosed area of the cross section. Note that the case of the uniform box beam is a special case of Equation (51). T_o , as given by Equation (47), assumes that shear buckling does not occur and, to account for such instability, some modifications of (51) are necessary as is discussed in the following subsection.

2. Failure Due to Shear Instability and Buckling

It is postulated here that, as in the case of the bending moment, the ultimate strength of a closed-deck hull under torsion, taking into consideration the effect of shear buckling, can be written in the form:

$$T_{b_o} = 2t \frac{\sigma_y}{\beta} \phi A_T \quad (52)$$

where ϕ is shear instability reduction factor defined as:

$$\phi = \frac{\tau_c}{\sigma_y/\beta} \quad (53)$$

τ_c is the shear failure stress which will be examined in subsections (a) and (b) below.

a. Plating Between Stiffeners

Consider the plating of a hull girder between stiffeners and loaded in shear at the four edges. Timoshenko [16] presents an approximate solution to the elastic buckling problem for this plate based on stationary potential energy considerations and using the Ritz method. The critical value of the shear stress is given by the usual formula:

$$\tau_{ce} = \frac{\pi^2 E}{12(1-\nu^2)} \left(\frac{t}{b}\right)^2 k \quad (54)$$

where k is the plate factor. This factor is dependent on the boundary conditions and the aspect ratio α . Bleich [24] gives simplified design formulae for k for various boundary conditions. For the simply supported case, k is given by:

$$k = 5.34 + \frac{4}{\alpha^2} \quad (\text{for } \alpha > 1)$$

where $\alpha = a/b$

The occurrence of plate instability is independent on the sense of the shear stress. Hence, for α to be larger than unity, one may select "a" as the larger dimension.

In the inelastic range, the principal stresses corresponding to a state of pure shear are all equal in magnitude to the shear stress. Bleich [24] points out that, as a consequence, it would be reasonable to assume isotropic plate behaviour in the inelastic range. The implication then is that a plasticity reduction factor approach may be used as in the axial compression case to compute the critical shear stresses in the inelastic range. Hence, we may write:

$$\tau_c = \tau_{ce} \cdot \eta \quad (55)$$

where η is the plasticity factor < 1 when τ_c is above the proportional limit. In Equation (55), if one substitutes ,

$$\eta = \sqrt{\tau} = \sqrt{\frac{E_t}{E}}$$

whose use is justified by Bleich on the basis of Stowell's experimental data, interpreted using the von Mises' yield criterion, we have:

$$\frac{\sigma_i}{\sqrt{\tau}} = \tau_{ce} \cdot \sqrt{3} \quad (56)$$

This expression implicitly uses $\sigma_i = \sqrt{3} \tau_c$ where σ_i is the intensity of stress according to the Huber, Mises, and Henkey plasticity hypothesis. [See Appendix I.]

To find the critical shear stress, one then computes $\sigma_i/\sqrt{\tau}$ from the above equation and obtains σ_i and hence τ_c from a tabulated relationship [e.g., Ref. 24, p. 343] between σ and $\sigma/\sqrt{\tau}$. Such tables can be prepared for a given material defined by its yield point and proportional limit. The Ostinfeld-Bleich parabola may be used for the ratio E_t/E .

A large deflection nonlinear solution for the case of a simply supported plate with boundary stiffeners and edge loaded in shear has been analyzed by Payer [33]. That solution is based on Marguerre's differential equations and includes the effect of initial imperfections. Design charts

for the two aspect ratios of 1.0 and 2.5 are presented. These charts cover a load range of up to 1.5 times the elastic critical shear stress. The extreme values of an equivalent surface stress, (including the effects of both bending and membrane stresses and based on the Huber-Mises-Henkey plasticity hypothesis concept of an equivalent uniaxial stress) the principal membrane stresses, and the plate bending stresses that come into play in the post-buckling range are given therein [33].

The results indicate that [33] surface stresses due to a combination of membrane and bending stresses may cause yielding in areas of the plate where the membrane stresses alone are still within the elastic range. If a certain amount of surface yielding is acceptable, then a consideration of the diagonal tension field due to membrane stresses alone may suffice. This conclusion was drawn for deep-web-frame plate panels, of low slenderness ratio, simple supported and edges kept straight. It should be noted, however, that the range of aspect ratios for shear-loaded panels at the deck or bottom in a typical longitudinally framed vessel is probably greater, and the plate slenderness higher than those given in Reference [33].

b. Stiffened Plates with One or More Longitudinal Stiffeners

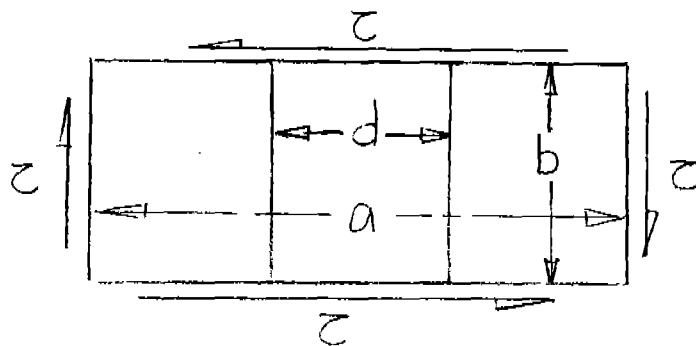


FIGURE 8. Stiffened Panel Under Shear

Timoshenko [34] solved the problem of the shear-loaded panel with either one or two stiffeners (see Figure 8) by means of an energy method and assuming that the stiffeners have no torsional stiffness. For the simply supported plate panel in pure shear, with

$$\alpha = \frac{d}{b} < 1$$

the plate factor to be used in Equation (54) is given by:

$$k = 4 + \frac{5.34}{\alpha^2}$$

Using the non-dimensional parameter:

$$\gamma = \frac{EI}{dD} = \frac{12(1-\nu^2) I}{t^3 d}$$

where I is the moment of inertia of the stiffener alone, Timoshenko determined the values γ_0 of the parameter γ which are required to ensure the critical stress given by the single panel Equation (54) with plate factor given above. Wang [35] extended Timoshenko's analysis to plates reinforced by any number of stiffeners. The value of γ_0 depends on d/b and may be found in Bleich [24, p. 415].

The solutions of both Timoshenko and Wang were based on a double sine series displacement function which Stern and Fralich [36] indicate as not suitable to express the deformation of a stiffened plate with a limited number of terms. Their own solution for simply supported infinitely long plates reinforced by equally spaced stiffeners was based on the Lagrangian multiplier method and the stationarity of the potential energy formulation. From their results, a design equation for the plate factor k , showing it as a function of the stiffener ratio γ and of the aspect ratio $\alpha = b/d$, is given by Bleich [24, p. 416]. It is:

$$k = 5.34 + (5.5 \alpha^2 - 0.6) \sqrt{3 \frac{\gamma}{4(7 \alpha^2 - 5)}}$$

valid for,

$$1 \leq \alpha \leq 5 \quad \text{and} \quad 0 \leq \gamma / (7 \alpha^2 - 5) \leq 4$$

If $\gamma > 4(7 \alpha^2 - 5)$, the plate factor is practically independent of γ and may be computed from,

$$k = 4.74 + 5.5 \alpha^2$$

These plate factors are to be used in conjunction with Equation (54).

Extension of the above results into the inelastic range may be accomplished by the plasticity reduction-factor approach suggested by Bleich [24].

It should be noted, however, that the torsional moment alone would probably not constitute a governing failure mode for closed-deck vessels where the ultimate torsional moment is about an order of magnitude greater than the expected service torsional load. For this reason, we will investigate next the effect of the torsional moment interacting with the vertical moment.

B. Development of Interaction Relations for Torsional and Vertical Moments

1. Fully Plastic Collapse--Yield Curve for Combined Bending and Torsion

Unlike the case of pure torsion, there exists no exact solution to this problem, although it has been shown [37] that the problem reduces to the solution of a certain nonlinear differential equation. In Ref. [14], Hodge uses the Theorems of Limit Analysis (see Appendix II) to obtain upper and lower bounds to the yield curve for a general beam case.

a. Lower Bound

Considering the shear stress distribution as in the case of pure torsion, but of reduced magnitude, one may write:

$$\tau^2 = (\tau_x^2 + \tau_y^2) < \left(\frac{\sigma}{\beta}\right)^2 \quad (57)$$

and the corresponding non-dimensional torque is given by:

$$t = \frac{T}{T_0} = \frac{\tau}{(\sigma_y/\beta)} \quad (58)$$

Acting together with this, is the normal stress σ similar to that in pure plastic bending, but of reduced magnitude ($\sigma < \sigma_y$). The non-dimensional bending moment is given by:

$$m = \frac{M}{M_0} = \frac{\sigma}{\sigma_y} \quad (59)$$

The best lower bound is obtained when,

$$\sigma^2 + \beta^2 \tau^2 = \sigma_y^2 \quad (60)$$

Combining Equations (58), (59), and (60) yields the approximate interaction relation.

$$m^2 + t^2 = 1 \quad (61)$$

A statically admissible stress distribution that is in equilibrium and does not violate the yield condition may be associated with any stress resultants m and t which lie in or on the circle defined by the interaction relation (61) given above. Therefore, this relation provides a lower bound for the yield curve.

b. An Upper Bound

Hill and Seibel [38] have constructed an upper bound for the yield curve. Considering symmetric sections and based on the rate of energy dissipation, one may obtain the following stress resultants for any cross section:

$$m = \frac{1}{M_0} \int_A \sigma y \, dA = \frac{\sigma_y}{M_0} \int_A \frac{y^2 \, dA}{[y^2 + w^2(x^2 + y^2)]^{\frac{1}{2}}} \quad (62)$$

$$t = \frac{1}{T_0} \int_A (x\tau_y - y\tau_x) \, dA = \frac{\sigma_y w}{\beta T_0} \int_A \frac{(x^2 + y^2) \, dA}{[y^2 + w^2(x^2 + y^2)]^{\frac{1}{2}}}$$

where w is a parameter. These stress resultants may be evaluated for any given section as functions of the parameter w . As an example, these Equations (62) were evaluated for a circular bar and for a square bar in Reference [14]. The maximum difference between the upper and lower bounds is less than 14% for the square section and 4% for the circular. Hence, the simple computation using the lower bound is suggested as sufficient for practical purposes. The upper bound can be only numerically evaluated for a hull girder using Equations (62). Figure 9 shows the interaction relation between the moment and the torque based on the lower bound which is conservative by about 10%.

2. Instability Collapse--The Shear Loaded Plate Subject to Uniform Edge Compression

a. Plating Between Stiffeners

Under the combined action of vertical and torsional moments, one typically has the deck or bottom plate panel loaded in both shear and compression as shown in Figure 10.

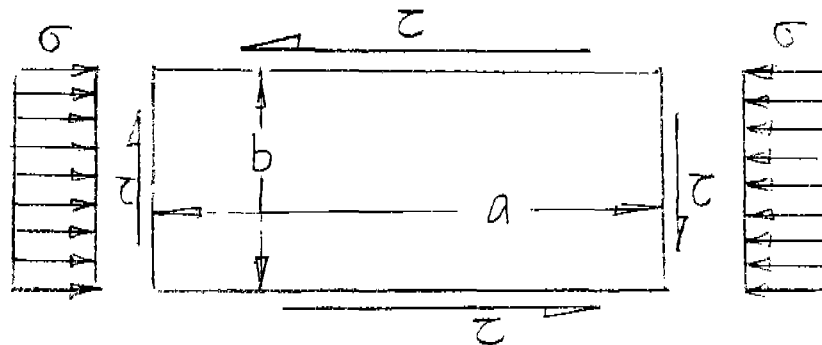


FIGURE 10. Plate Under Compression and Shear

Here we consider the effect of such a load combination on the stability of the plate panel. This problem lends itself to a stationary potential energy solution by the Ritz method. Results presented by Bleich [24, p. 404] are shown in Figure 11 in the form of interaction relationships. Note that τ_0 is the elastic critical stress in pure shear and σ_0 , the elastic critical stress in pure compression. These results may also be given in terms of

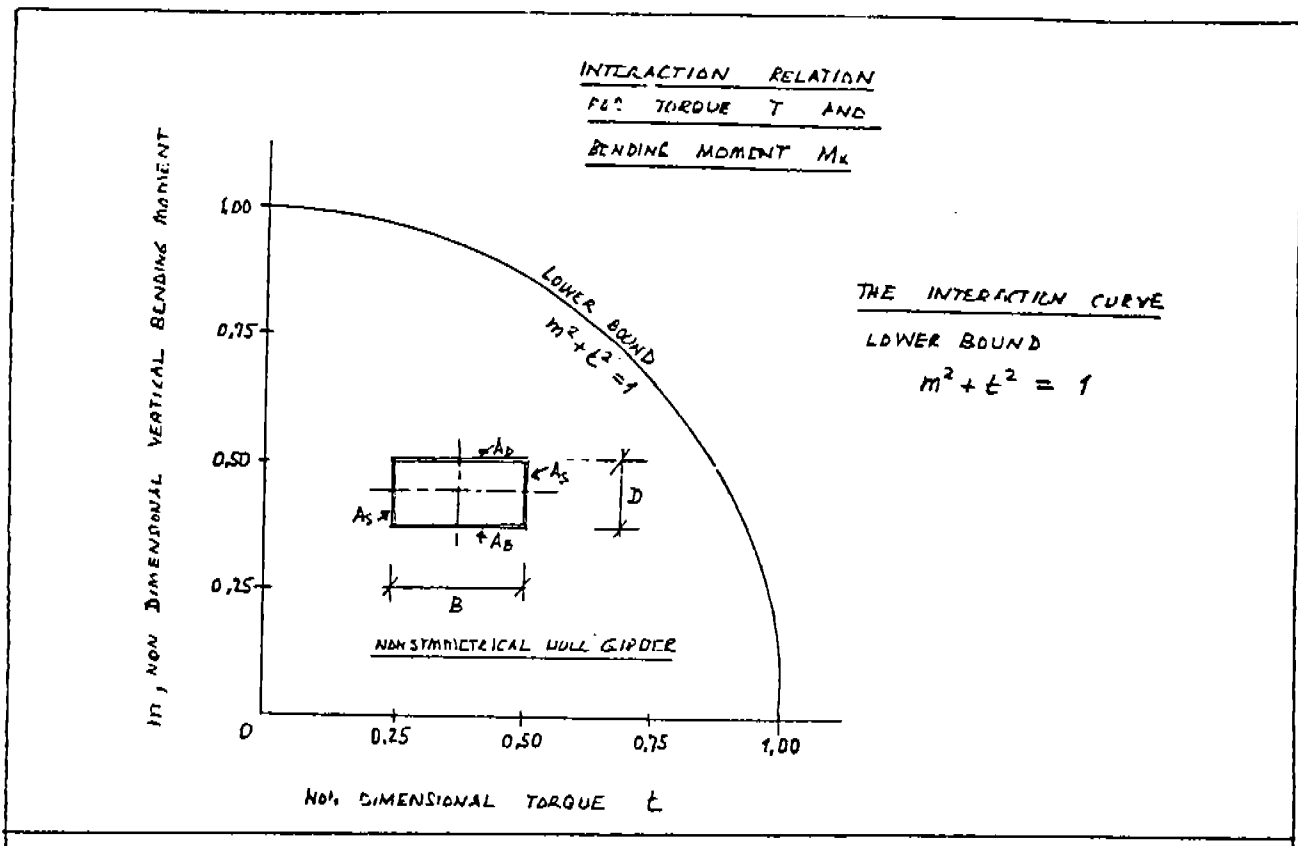


FIGURE 9. Interaction Curve Under Vertical and Torsional Moments

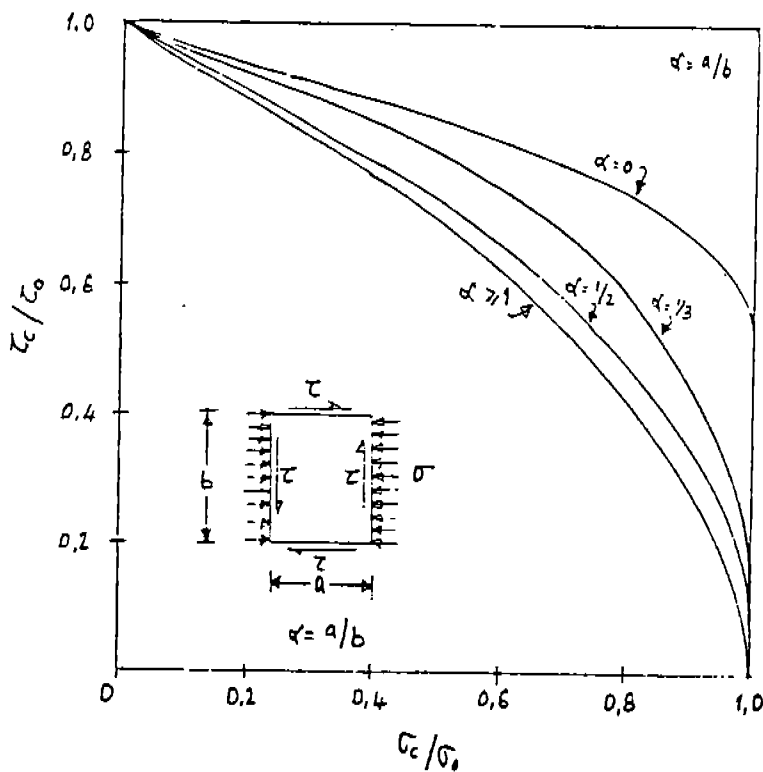


FIGURE 11.

Stability Interaction Curves
for Plates Under Compression
and Shear

design formulae. Reference [24] gives the following equations for long plates, $\alpha > 1$ in the elastic range:

With $\delta = \sigma_c / \tau_c$

$$\tau_c = \frac{\pi^2 E}{12(1-\nu^2)} \left(\frac{t}{b}\right)^2 2 \delta k^2 \left(-1 + \sqrt{1 + \frac{4}{\delta^2 k^2}}\right) \quad (63)$$

where,

$$k = \frac{4}{3} + \frac{1}{\alpha^2}$$

For extension into the inelastic range, one assumes the plasticity factor $\eta = \sqrt{\tau}$ is dependent on von Mises' equivalent uniaxial stress intensity given in this case by:

$$\sigma_i = \sqrt{\sigma_c^2 + 3 \tau_c^2}$$

Introducing $\delta = \sigma_c / \tau_c$ and replacing E by $E \sqrt{\tau}$ we obtain:

$$\frac{\sigma_i}{\sqrt{\tau}} = \frac{\pi^2 E}{12(1-\nu^2)} \left(\frac{t}{b}\right)^2 2 \delta k^2 \sqrt{\delta^2 + 3} \left(-1 + \sqrt{1 + \frac{4}{\delta^2 k^2}}\right) \quad (64)$$

One computes $\sigma_i / \sqrt{\tau}$ and obtains σ_i depending on τ as is usual. The critical stresses are then,

$$\tau_c = \frac{\sigma_i}{\sqrt{\delta^2 + 3}} \quad \text{and} \quad \sigma_c = \frac{\delta \sigma_i}{\sqrt{\delta^2 + 3}} \quad (65)$$

Similar design formulae for the case of the wide plate, both for the elastic and the small-deflection plastic case, may be obtained from Bleich [24, p. 406]. For the post-buckling solution and including material non-linearities, one should refer to the method suggested in Reference [33] using Marguerre's equations.

b. Stiffened Plates Under Uniform Edge Compression and Edge Shear

For the case of the stiffened plate with one or two longitudinal stiffeners, there seems to be no practical solution available at the present time. For the case of three or more stiffeners in the pre-buckling and post-

buckling ranges, one may use the results given in [15]. The numerical solutions given therein to the orthotropic plate theory equations developed in [39] are limited to cases where the edge shear is less than the critical value of the edge shear when the shear load is applied alone on the same panel.

V. ULTIMATE STRENGTH UNDER COMBINED VERTICAL, LATERAL AND TORSIONAL MOMENTS

The effects of the presence of lateral and torsional moments on the vertical collapse bending moment are discussed in this section. In part "A" of the section, a suitable analysis procedure is proposed and in part "B", the procedure is applied to a large tanker in order to illustrate its details.

A. A Suitable Evaluation Procedure and Interaction Relations

As in the previous sections, two separate major modes of failure are considered here: (1) failure to yielding and plastic flow; and (2) failure resulting from major instability and buckling of grillages making up the hull sections.

1. Failure Due to Yielding and Plastic Flow

An interaction relation is developed here for a hull girder subjected to vertical, lateral, and torsional moments. Since the exact solution to this problem is difficult, only bounds on the yield surface from below and above will be constructed using theorems of limit analysis (see Appendix II).

a. Lower Bound

It is assumed here that the distribution of the normal stress σ is similar to that encountered in pure bending [14]. Thus, tensile and compressive stresses of magnitude " σ " are distributed as in the absence of twist (see Equation (42)) but the magnitude is such that:

$$m_x \frac{\sigma_y}{\sigma} + k (m_y \frac{\sigma_y}{\sigma})^2 = 1 \quad |m_y| < |m_x| \quad (66)$$

where k for the general unsymmetrical girder is given by (see Equation (43)):

$$k = \frac{(A + 2 A_S)^2}{16 A_S (A - A_S) - 4 (A_D - A_B)^2}$$

The shear-stress distribution is similar to that in pure torsion but of magnitude τ_s . The dimensionless torque is given by:

$$t = \frac{T}{T_0} = \frac{\beta \tau_s}{\sigma_y} \quad (67)$$

τ_s and σ are related such that the yield condition is satisfied.

$$\sigma^2 + \beta^2 \tau_s^2 = \sigma_y^2 \quad (68)$$

Eliminating τ_s and σ from Equations (66), (67), and (68), one obtains the following interaction relation between m_x , m_y and t :

$$k m_y^2 + m_x \sqrt{1-t^2} + t^2 = 1 \quad |m_y| < |m_x| \quad (69)$$

In Equation (69) the following terms are defined:

$$m_x = \frac{M_x}{M_{x_0}} \quad ; \quad m_y = \frac{M_y}{M_{y_0}} \quad ; \quad t = \frac{T}{T_0}$$

$$k = \frac{(A + 2 A_s)^2}{16 A_s (A - A_s) - 4 (A_D - A_B)^2}$$

$$A = A_D + A_B + 2 A_s \quad ; \quad \frac{g}{D} = \frac{A - 2A_D}{4A_s} \quad (70)$$

$$M_{x_0} = \sigma_y [A_D g + A_B (D-g) + 2A_s (\frac{D}{2} - g + \frac{g^2}{D})]$$

$$M_{y_0} = \sigma_y [A_s B + \frac{B}{4} (A_D + A_B)]$$

$$T_0 = 2 \frac{\sigma_y}{\beta} t \cdot A_T$$

$$A_T = B \times D = \text{enclosed area of section of breadth } B \text{ and depth } D$$

$$t = \min. (t_D, t_s, t_B) = \text{minimum thickness of deck, side or bottom, respectively.}$$

$$\beta = 2 \text{ Tresca}$$

$$= \sqrt{3} \text{ von Mises}$$

As a special case, for a symmetric section, i.e., $A_D = A_B = A_f$, Equation (69) remains to have the same form but with variables defined as follows:

$$k = \frac{(1 + \frac{1}{2c})^2}{(1 + \frac{2}{c})} \quad ; \quad c = \frac{A_s}{A_f} \quad (71)$$

$$M_{x_0} = \sigma_y A_f D (1 + \frac{c}{2})$$

$$M_{y_0} = \sigma_y A_s B (1 + \frac{1}{2c})$$

The other variables, not appearing in Equation (71), are defined by Equation (70). Notice that Equations (69) and (70) reduce to Equations (42) and (43) when substituting $t=0$ for the special case of interaction between two bending moments only.

For a given ship particulars, i.e., A_D , A_S , A_B , B , D , σ_y , and a given value of the maximum lateral moment M_y , one may determine k , M_{x0} , M_{y0} , T_0 , m_y , and t using Equation (70). Then from the interaction relation Equation (69), one may determine m_x and M_x , i.e., the fully plastic yield moment when the vessel is subject to combined vertical, lateral, and torsional moments. Figure 12 shows the interaction relations (69) for different values of t .

An interaction relation (lower bound) can be also determined for the case when $|m_y| \geq |m_x|$; however, such a case is not realistic in actual ships.

b. Upper Bound

An upper bound yield surface can be determined from energy considerations [14]. For any cross section, the upper bound yield surface is given by:

$$\begin{aligned}
 m_x &= \frac{\sigma_y}{M_{x0}} \int_A \frac{x (w_1 x + w_2 y)}{[x^2 + y^2 + (w_1 x + w_2 y)^2]^{\frac{1}{2}}} dA \\
 m_y &= \frac{\sigma_y}{M_{y0}} \int_A \frac{y (w_1 x + w_2 y)}{[x^2 + y^2 + (w_1 x + w_2 y)^2]^{\frac{1}{2}}} dA \\
 t &= \frac{\sigma_y}{\beta T_0} \int_A \frac{(x^2 + y^2)}{[x^2 + y^2 + (w_1 x + w_2 y)^2]^{\frac{1}{2}}} dA
 \end{aligned} \tag{72}$$

The yield surface is defined in terms of two parameters w_1 and w_2 . Unfortunately, the integrals in Equation (72) cannot be conveniently evaluated even for the simpler cross sections. For all practical purposes however, it is sufficient to use the conservative lower-bound relation given by Equation (69).

If shakedown analysis is performed (see Section II-B-2), it is recommended that M_x , as determined from Equation (69), be used to replace M_{x0} in the right hand side of inequalities (16) and (17) in order to include the effects of the lateral and torsional moments.

2. Failure Resulting from Major Instability and Buckling

This important mode of failure was analyzed in detail in Section II-C of this report. In the present section, only the effects of the lateral and torsional moments on the failure stress ratio ϕ as used in Equations (20) and (21) will be investigated. These Equations (20) and (21), may still be used

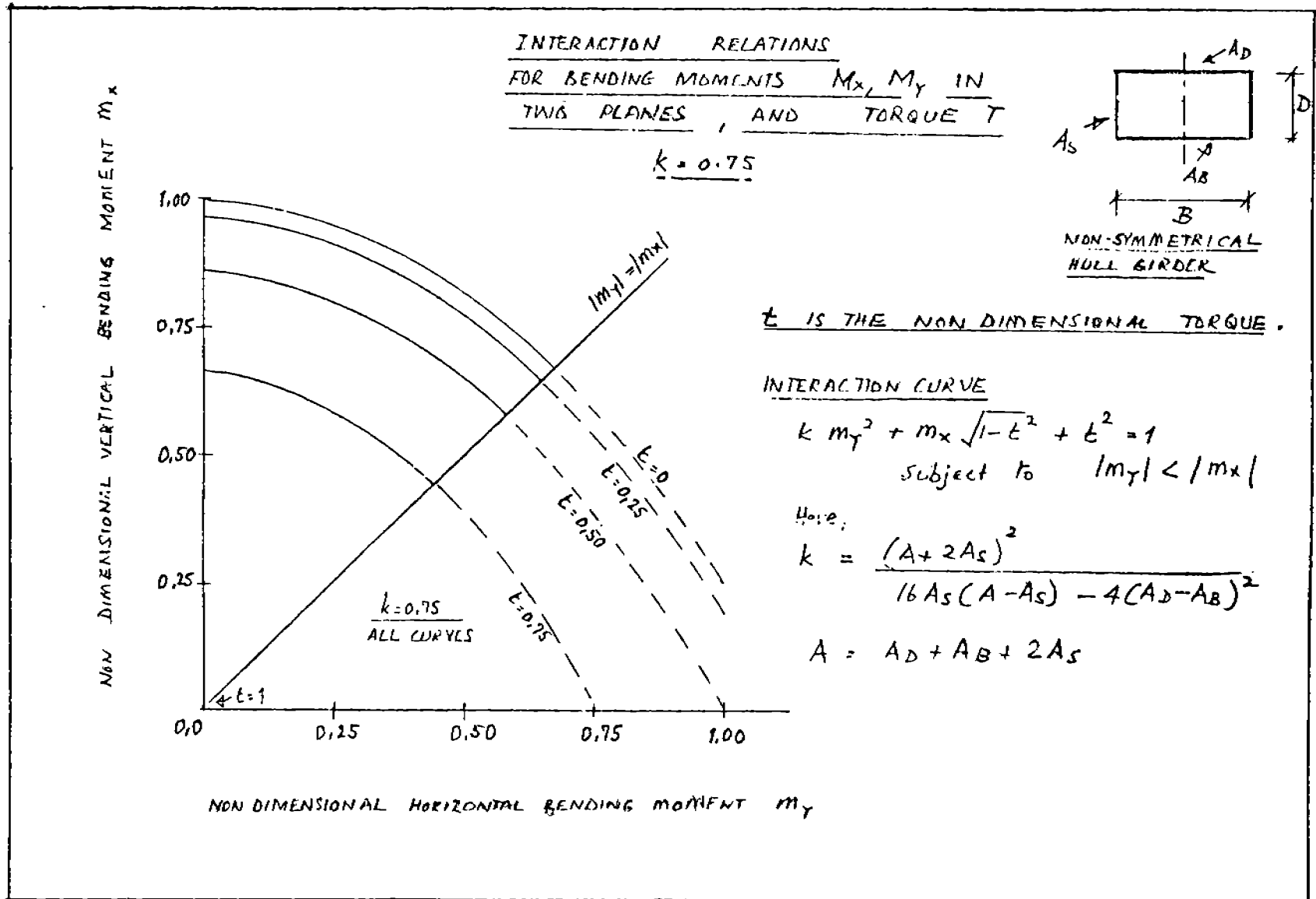


FIGURE 12. Interaction Curves Under Vertical, Lateral, and Torsional Moments

under the present load combination in order to determine the load-carrying capacity of the hull. However, the values assumed by the non-dimensional failure stress ϕ in the different buckling modes of failure should be calculated to reflect the edge loading condition of the plating (stiffened and unstiffened) under such load combination.

a. Unstiffened Plates

In general, when the hull girder is subjected to vertical, lateral, and torsional moments, unstiffened as well as stiffened plates in deck, bottom, and side grillages will be subjected to non-uniform axial compression together with edge shear as shown in Figure 13.

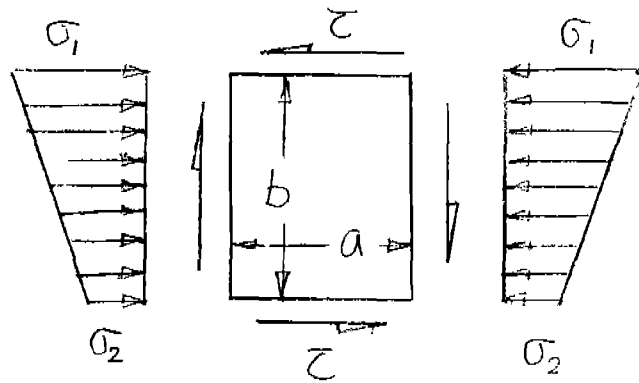


FIGURE 13. Plate Under Non-Uniform Compression and Edge Shear

For the case of unstiffened plates, the following equation for the elastic and inelastic buckling may be used:

$$\frac{\sigma_i}{\sqrt{\tau}} = 26750 \left(\frac{t}{b}\right)^2 k \quad \text{for steel} \quad (73)$$

and

$$\tau_c = \text{critical shear buckling stress} = \frac{\sigma_i}{\sqrt{\beta^2 + 3}}$$

$$\sigma_{1c} = \text{critical compressive buckling stress at one edge of the plate (see Figure 13)} = \frac{\beta \sigma_i}{\sqrt{\beta^2 + 3}}$$

where

$$\beta = \frac{\sigma_1}{\tau_{xy}} \quad ; \quad \tau_{xy} = \text{edge shear (Fig. 13)}$$

$$\tau = \text{plasticity factor} = \frac{E_t}{E}$$

E_t = tangent modulus of the material

t, b = plate thickness and breadth, respectively

k = factor which depends on the ratio of σ_1 to σ_2
(see Fig. 13) and the boundary conditions.

Bleich [24] in Table 36, p. 412 gives the necessary equations for determining the factor k for the cases when $\sigma_2 = 0$ and $\sigma_1 = -\sigma_2$ of a simply supported plate. Figure 14 shows the interaction relation as developed by Timoshenko for simply supported plates under pure inplane bending and boundary shear (see Reference [24], p. 407).

b. Stiffened Plates

A gross panel in the deck bottom will be subject to an edge loading condition as shown in Figure 13 when the hull girder is under combined vertical, lateral, and torsional moments. For the case of a plate stiffened by one or two stiffeners, Bleich [24, p. 424] discusses the buckling strength when $\sigma_1 = -\sigma_2$. Unfortunately, for the more general case, where $\sigma_1 \neq -\sigma_2$, no solution is given. It is suggested, however, that such non-uniform compressive loads shown in Figure 13 can be replaced by a statically equivalent uniform edge compressive load. Using such simplification, the formulations and references given in Section IV-B-2 may be used to determine the buckling strength.

In the case of a uniform grillage with several stiffeners, References [7,15] may be used for determining the ultimate strength under a statically equivalent uniform edge compression and edge shear. The charts given in these references account also for the effects of lateral loads on the grillage and a biaxial edge compression.

It should be noted that the panel buckling modes (flexural and tripping buckling of stiffener) will not be strongly affected by the presence of lateral and torsional moments acting on the hull girder. Therefore, the analysis and formulations given in Section I-C-2 may be considered adequate for evaluating panel buckling failure under combined moments.

B. Application to a Tanker

The following example serves to illustrate the calculation of the ultimate longitudinal bending moment for a ship hull girder and are developed in three parts:

1. The Computation of the Fully Plastic Bending Moment With Buckling Effects Excluded.
2. Investigation of Buckling Instability and the Determination of Strength Reduction Factors Due to Compressive Buckling.
3. Evaluation of the Governing Mode of Failure and the Estimation of the Ultimate Strength of the Hull.

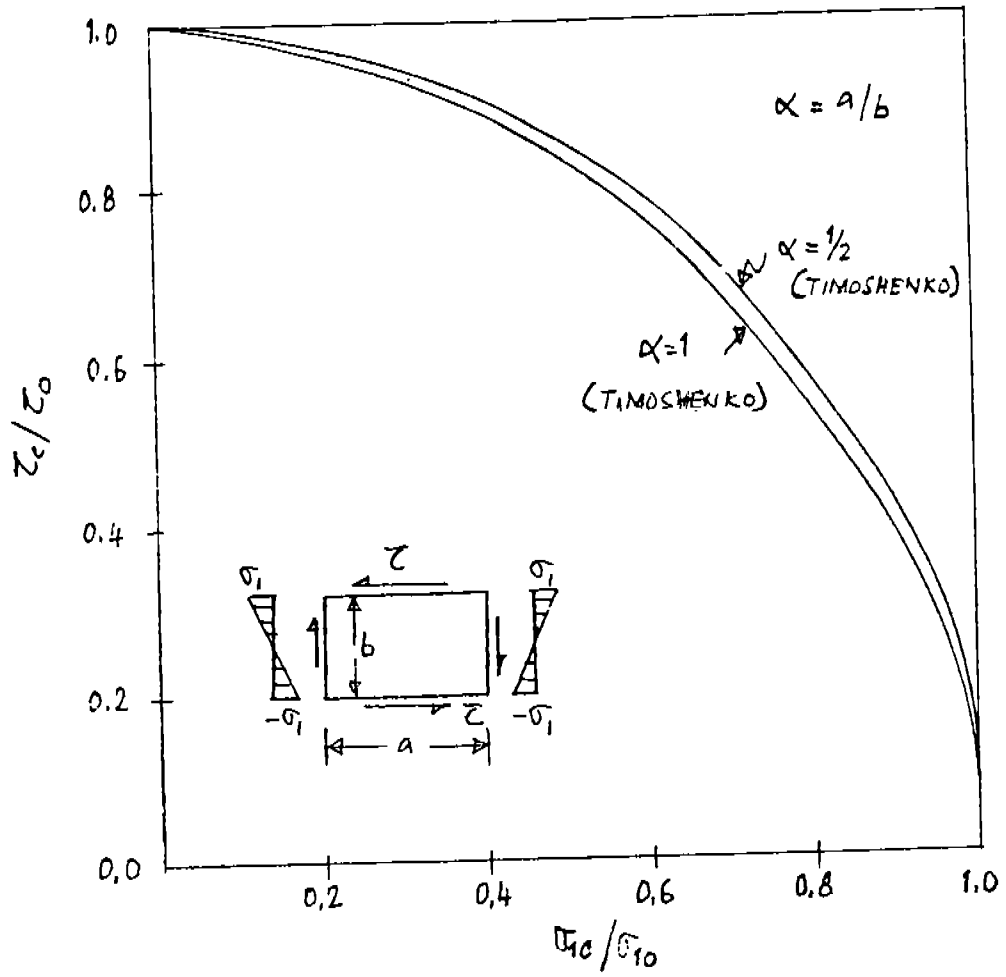


FIGURE 14. Plate Under Inplane Bending and Edge Shear

1. Computation of the Fully Plastic Bending Moment for a Tanker, With Buckling Effects Excluded

The analysis developed in this paper is now applied to a 200,000 ton displacement tanker illustration. The principal particulars of the tanker are:

$$L_{pp} = 1000 \text{ ft.}$$

$$B = 155 \text{ ft.}$$

$$D = 78 \text{ ft.}$$

$$C_{\beta} = 0.821 \text{ at } 55.5 \text{ ft. draft}$$

The following geometric properties were computed from the tanker's midship section:

$$A_D = 31.78 \text{ ft.}^2 \qquad t_D = 2.46 \text{ in.}$$

$$A_B = 29.71 \text{ ft.}^2 \qquad t_B = 2.30 \text{ in.}$$

$$A_S = 17.75 \text{ ft.}^2 \qquad t_S = 2.73 \text{ in.}$$

$$\begin{aligned} A &= A_D + A_B + 2 A_S \\ &= 97.00 \text{ ft.}^2 \end{aligned}$$

In idealizing the cross section, the longitudinal bulkheads present were diffused with the sides. All longitudinal stiffening was appropriately diffused. Assuming that the cross section is stable, we now proceed to calculate the fully plastic bending moment for the above hull girder.

a. The Vertical Bending Moment

For this loading, the distance "g" of the plastic neutral axis below the deck, as the horizontal line that divides the cross section into two equal areas, is given by:

$$g = \left[\frac{2 A_S + A_B - A_D}{4 A_S} \right] D = 36.73 \text{ ft.}$$

Assuming a material yield stress of 34 ksi (15.17 t/in) in both tension and compression, one may then obtain the fully plastic yield moment M_{X_0} if the vertical bending moment were to act alone:

$$\begin{aligned} M_{X_0} &= \sigma_y \left[A_D g + A_B (D-g) + 2 A_S \left(\frac{D}{2} - g + \frac{g^2}{D} \right) \right] \\ &= 6.751 \times 10^6 \text{ ft.-tons} \end{aligned}$$

The design hull girder bending moment M_x for purposes of our illustration was obtained from Section 6 of the ABS Steel Vessel Rules, 1978, by adding a still-water bending moment of 1.486×10^6 ft.-tons to a wave bending moment of 2.459×10^6 ft.-tons. This yields:

$$M_x = 3.945 \times 10^6 \text{ ft.-tons}$$

Thus, we have the non-dimensional vertical bending moment ratio:

$$m_x = \frac{M_x}{M_{x0}} = 0.5844$$

b. The Lateral Bending Moment

If the lateral bending moment were to act alone, the fully plastic yield moment is:

$$\begin{aligned} M_{y0} &= \sigma_y \left[A_s B + \frac{B}{4} (A_D + A_B) \right] \\ &= 11.962 \times 10^6 \text{ ft.-tons} \end{aligned}$$

If one assumes conservatively a service lateral bending moment M_y of the same magnitude as the design vertical bending moment, one obtains the horizontal bending moment ratio:

$$m_y = \frac{M_y}{M_{y0}} = 0.3298$$

It should be noted that M_{y0} is much larger than M_{x0} ($M_{y0} = 1.77 M_{x0}$).

c. The Torsional Loading

The torque " T_0 " that causes fully plastic yielding for the cross section is given by:

$$T_0 = \frac{2 \sigma_y}{\beta} t A_T$$

where

$$\beta = \text{a shear yield criterion} = 2 \text{ (Tresca)}$$

$$t = \min (t_s, t_B, t_D) = 2.30 \text{ in.}$$

$$A_T = \text{enclosed area} = B \times D$$

Thus,

$$T_0 = 5.066 \times 10^6 \text{ ft.-tons}$$

The torque encountered during service may be estimated by an expression due to Vedeler [31, p. 196]:

$$T = \frac{C LB^3}{3500}, \quad C = 0.35$$

$$= 3.724 \times 10^5 \text{ ft.-tons}$$

Hence, we have the non-dimensional torque ratio:

$$t = \frac{T}{T_0} = 0.0735$$

"t" is thus very small and its effect, in this case, is expected to be negligible.

d. Effect of the Vertical Shear Force

The shear force S_0 causing fully plastic yield is given for the case of a symmetrical cross section ($A_D = A_B = A_f$) by

$$S_0 = \frac{2 \sigma_y}{\beta} A_S$$

$$= 38,802 \text{ tons}$$

A design shear force of 12,110 tons obtained from the ABS Steel rules may then be used to obtain the shear force ratio:

$$s = \frac{S}{S_0} = 0.312$$

e. Effect of the Axial Force

The maximum service axial force for the tanker was estimated to cause an axial stress of 60 lb/in² which is negligible compared to the bending and shear stresses and to the fully plastic axial stress, i.e., the yield stress.

Using the above dimensionless loads, one may now assess the effect of their interactions on the vertical bending strength.

i. For the case of the vertical bending moment interacting with the lateral moment, we have the yield relation:

$$k m_y^2 + m_x = 1 \quad ; \quad |m_x| \geq |m_y|$$

where

$$k = \frac{(A + 2 A_S)^2}{16 A_S(A - A_S) - 4 (A_D - A_B)^2} = 0.781$$

With $m_y = 0.3298$, we obtain $m_x = 0.915$.

ii. If torque acts together with bending in two orthogonal planes, we have the relation:

$$k m_y^2 + m_x \sqrt{1-t^2} + t^2 = 1 ; |m_x| \geq |m_y|$$

With $m_y = 0.3298$ and $t = 0.0735$, we have $m_x = 0.912$.

iii. If the hypothetical case where vertical bending moment and shear force act concurrently, using the wide-flange interaction curve as a conservative approximation, we have:

$$s^2 + m_x^2 = 1$$

This gives $m_x = 0.902$ for $s = 0.312$.

From the above calculations, we may conclude that while torque and axial force effects are negligible, the presence of the lateral bending moment or shear forces could reduce the vertical bending moment capacity of the hull girder by about 9 to 10 percent. It may, however, be noted that the maxima of the vertical bending moment and shear forces do not occur at the same location along the hull length. The maximum permissible vertical bending moment m_{xp} may then be taken as:

$$m_x = 0.912 ; M_x = 6.157 \times 10^6 \text{ ft.-tons}$$

A design value of $m_x = 0.584$ then implies a factor of safety of 1.56 based on the fully plastic ultimate strength. This may reduce further when the possibility of buckling is accounted for.

2. Investigation of The Buckling Instability of the Hull Cross Section

The determination of the true collapse moment must account for the possibility of buckling instability of the structural elements that constitute the hull girder. Here we consider the compressive strength of the weaker deck gross panel in order to assess this detrimental effect. A typical deck panel under investigation is shown in Figure 15.

The instability and buckling strength of (a) plate elements between stiffeners, (b) panel instability including flexural and tripping modes of failure, and (c) grillage instability leading to failure will be considered separately as follows.

a. Local Buckling of Plate Elements

The deck panel under investigation consists of plate elements that may buckle locally even before the inception of a primary instability. That would in turn affect the load-carrying capacity in the primary modes of failure. Related to this question of interaction, there exists the possibility that this load shirking by the plate may mean that the ultimate load for the gross panel may be reached before the stiffeners fail. We are

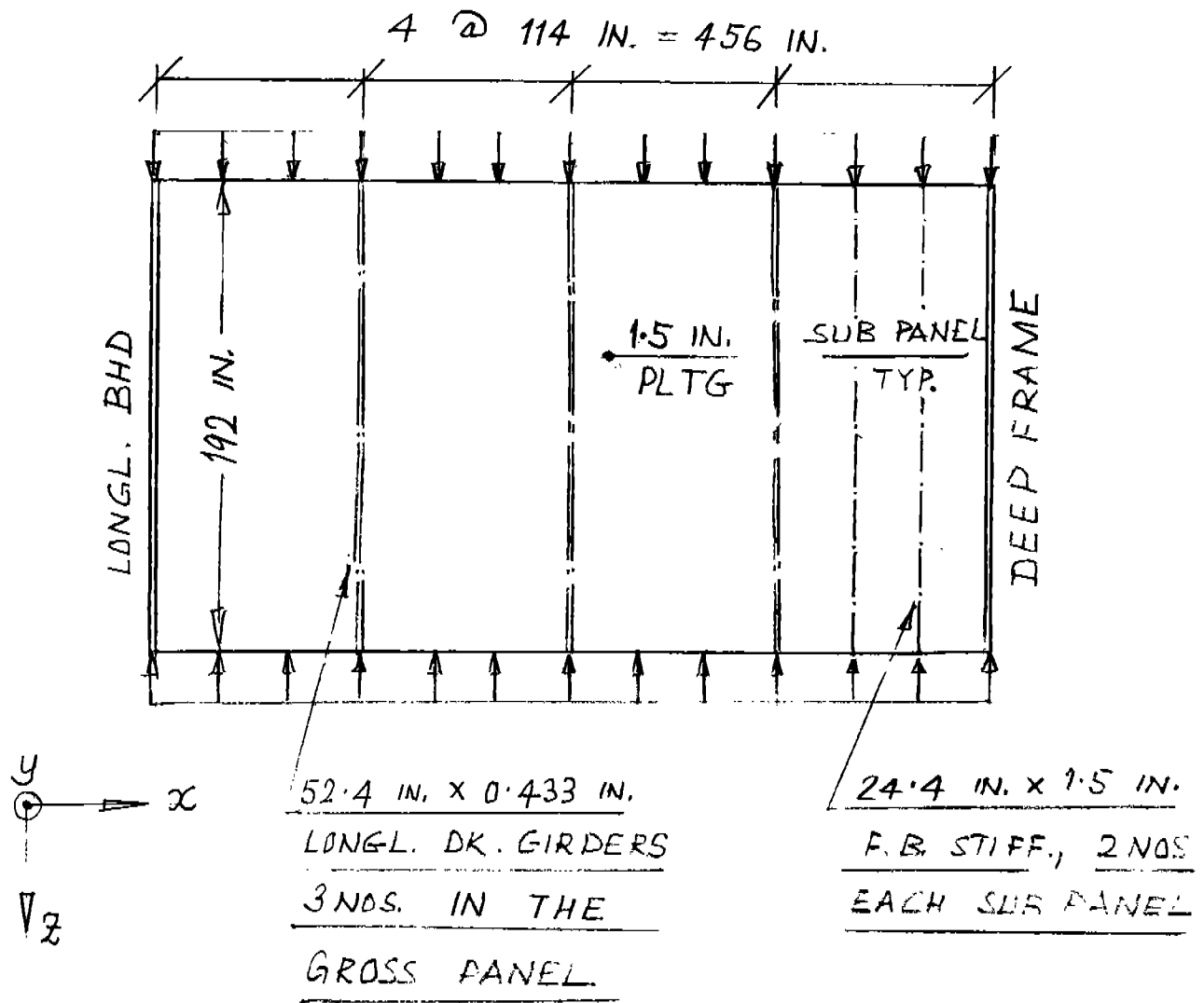


FIGURE 15. Deck Gross Panel of a Tanker

thus faced with the necessity of having to consider the instability and strength of plating both in the deck and in the web of deck girders in some detail.

i. A typical unstiffened plate panel in the deck is considered simply supported all around, under combined shear and uniformly distributed longitudinal stress (Figure 16):

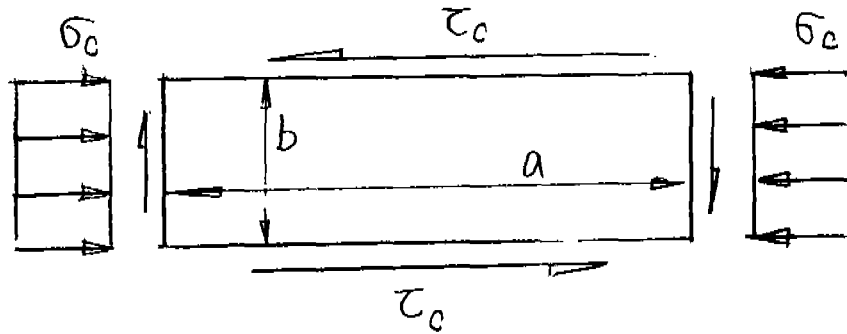


FIGURE 16. Plate Subjected to Uniform Compression and Edge Shear

The elastic critical stress in pure compression (σ_c^0) is given by [24, p. 320]:

$$\sigma_c^0 = k \frac{\pi^2 E}{12 (1-\nu^2)} \left(\frac{t}{b}\right)^2$$

For an aspect ratio of 5, the critical stress is a minimum for the plate buckling in 5 half waves, with a plate factor of $k = 4.0$. Using an elastic modulus E of 30,000 ksi, a Poisson ratio of 0.3 and the yield stress σ_{yp} of 34,000 ksi, we obtain:

$$\sigma_c^0 = 169 \text{ ksi} = 75 \text{ t/in}^2$$

The elastic critical stress in pure shear (τ_c^0) is considered next.

The occurrence of the plate instability under pure shear does not depend on the direction of the shear stress τ_c . The value of the critical stress may be determined from the usual formula, with a plate factor k given approximately by [24, p. 395]:

$$\begin{aligned} k &= 5.34 + \frac{4}{\alpha^2} \quad (\text{for } \alpha > 1) \\ &= 5.5 \end{aligned}$$

Hence,

$$\tau_c^0 = 232 \text{ ksi} = 104 \text{ t/in}^2$$

For the case of combined shear and longitudinal compression, we have an approximate parabolic interaction [24, p. 405]:

$$\left(\frac{\tau_c}{\tau_c^0}\right)^2 + \frac{\sigma_c}{\sigma_c^0} = 1$$

For the given hull, we previously obtained a maximum design shear force of 12110 tons. A calculation of shear flow in the deck assuming the centerline as a point of zero shear, gives a flow linearly increasing to 21.87 t/ft. at the longitudinal bulkhead, which is 40.7 ft. off centerline. τ_c calculated as an average over 38" on the maximum side is:

$$\tau_c = 2.62 \text{ ksi} = 1.17 \text{ t/in}^2$$

We thus have $(\tau_c/\tau_c^0)^2 = 0.00013$ and $\sigma_c = 0.9999 \sigma_c^0$. This reduction is negligible. One may also bear in mind that the maxima of the bending moment and shear force occur at different locations along the length.

From the load-shortening curves for near perfect plates with small residual stresses and initial deformations [21, p. 15], one may see that plating of the given slenderness $b/t = 25$ is not likely to fail until the average strain is well past the yield strain. The plating would thus remain a fully effective flange for the case of column behavior.

The critical longitudinal stress in the inelastic range (σ_c^i), neglecting the effect of shear, is given from [24, p. 343]:

$$\sigma_c^i / \sqrt{\tau} = \sigma_c^0$$

$\tau = E_t/E$ is a reduction factor related to plasticity. On using the Ostenfeld-Bleich parabola for τ together with an assumed proportional limit of 25 ksi and a yield strength of 34 ksi, we have:

$$\sigma_c^i = 33.74 \text{ ksi} = 0.99 \sigma_y$$

ii. Stability of the longitudinal deck girder web plate (Figure 17), considered simply supported, under longitudinal compression [24, p. 410]: Here we have an elastic critical stress $\sigma_c^0 = 57.02 \text{ ksi} = 25.45 \text{ t/in}^2$ based on a plate factor $k = 7.7$.

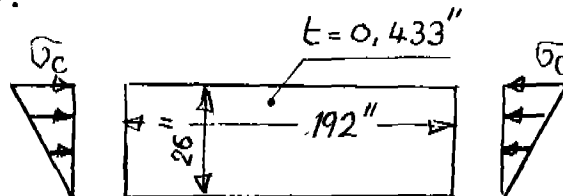


FIGURE 17. Web Plating

Neglecting the effect of shear and using the plasticity reduction factor approach, the critical stress in the inelastic range is then found to be:

$$\sigma_C^i = 31.8 \text{ ksi} = 0.94 \sigma_y$$

This value is probably on the conservative side because of the assumed simply supported boundary conditions.

iii. For the smaller 24.4" x 1.5" flat-bar stiffener, the possibility of local web buckling is thought not to be critical. For that case, assuming one end fixed and the other free, (plate factor $k = 1.277$), we obtain:

$$\sigma_C^0 = 131 \text{ ksi} = 58.4 \text{ t/in}^2$$

and,

$$\sigma_C^i = 33.6 \text{ ksi} = 0.99 \sigma_y$$

b. Panel Failure Mode Including Flexurel and Tripping

i. Flexural Buckling of Longitudinal Stiffening

The mode of failure considered is that of a purely flexural column collapse, with the stiffener and an effective width of plating comprising the cross section. Pinned ends are assumed. No account is taken of the presence of any lateral pressure. As an approximation, column formulas are used, with the column mode considered separately from any possible tripping.

The flat-bar stiffener. From the analysis of local buckling of plating, it is seen that because of its stockiness, very little load reduction, if any, is likely to occur in the flange. The plating comprising the flange is then fully effective throughout the range of column behaviour. The web has also been found stable.

Properties of the section shown in Figure 18 are:

Neutral axis 4.78" below flange.

$I =$ moment of inertia = 5129 in⁴

$A =$ area of the section = 93.6 in².

The Euler elastic buckling stress for the section is:

$$\sigma_{CE} = \frac{\pi^2 EI}{A l^2} = 440 \text{ ksi} = 196 \text{ t/in}^2$$

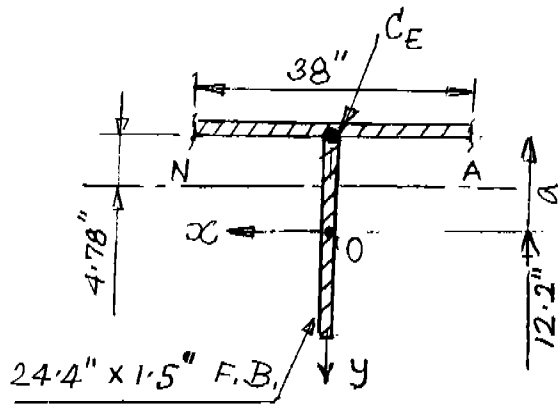


FIGURE 18. Flat Bar Deck Stiffener

For the inelastic case, if one uses a plasticity reduction-factor approach with E_t/E given by the Bleich parabola, together with a structural proportional limit of $0.5 \sigma_y$, one obtains [41, p. 54]:

$$\frac{\sigma_c}{\sigma_y} = 1 - 0.25 \lambda_{cE}^2, \quad 0 \leq \lambda_{cE} \leq \sqrt{2}$$

where

$$\lambda_{cE}^{-2} = \sigma_{cE} / \sigma_y = 12.74$$

Hence we have the critical stress:

$$\sigma_c = 33.3 \text{ ksi} = 14.88 \text{ t/in}^2 = 0.98 \sigma_y$$

The longitudinal deck girder. In the section shown in Figure 19, the top flange accounts for both the plating and diffused areas of the 24" x 1.5" FB stiffeners.

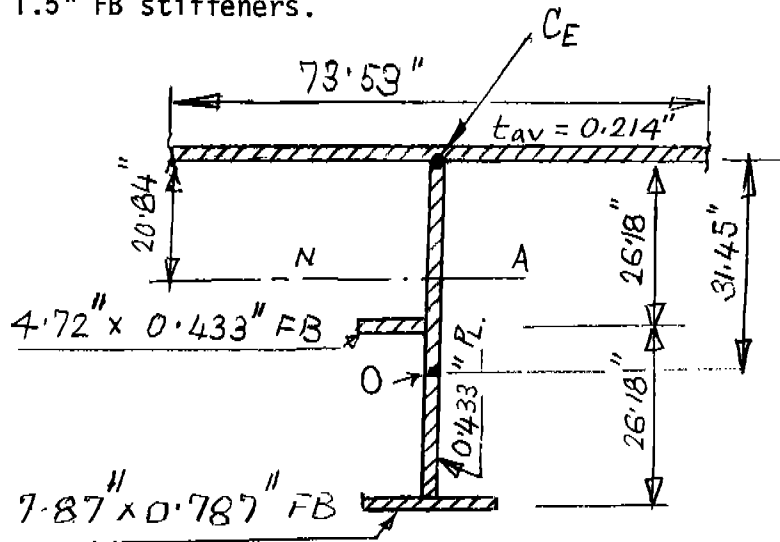


FIGURE 19. Deep Deck Girder

For the simply supported case of multiple webs, one may obtain an effective breadth of 0.645 times a spacing of 114". This accounts for shear-lag effects [42,43]. Other relevant section properties are:

$$I = \text{moment of inertia} = 18838 \text{ in}^4$$

$$A = \text{area of cross section} = 46.65 \text{ in}^2$$

On applying the formulae given before, one then obtains the following results for the elastic and small-deflection inelastic cases, respectively:

$$\sigma_{cE} = 3235 \text{ ksi} = 1444 \text{ t/in}^2$$

$$\sigma_c = 33.91 \text{ ksi} = 15.14 \text{ t/in}^2 = 0.997 \sigma_y$$

The possibility of local buckling may exist for the web, as is evident from previous analysis. This is not accounted for in this calculation.

ii. Lateral Torsional Buckling of Longitudinal Stiffening (Tripping)

The elastic critical stress causing tripping of the web of the columns being considered may be obtained from [24, p. 138]:

$$\sigma_{TE} = \frac{\pi^2 E}{(\ell/r_e)^2}$$

where ℓ is the length of the column between supports, and r_e an effective radius of gyration. We consider here the case of the section web and lower flange turning about an enforced axis of rotation, namely the intersection line with the plate. The plating which forms the upper flange is assumed to provide a restraint against this rotation. The plating is not expected to locally buckle according to the previous calculations and hence the rotational stiffness supplied by it is constant through the range of loading. The sections are assumed symmetrical. The possibility of web deformation is not accounted for. A small-deflection plastic extension to the inelastic range may be done in the same manner as for the case of the flexural buckling [41, p. 64] resulting in:

$$\sigma_T = \sigma_y - 0.25 \frac{\sigma_y^2}{\sigma_{TE}}, \quad \sigma_{TE} \geq 0.5 \sigma_y$$

This again assumes the Bleich parabola for E_t/E , together with a structural proportional limit σ_p of half the yield stress. Application of this procedure to the longitudinal stiffeners is shown below.

The flat-bar stiffener whose pinned ends are prevented from twisting; elastic critical stress. The minimum radius of gyration for this case is given from [24] by:

$$r_e^2 = \frac{\ell^2}{\pi^2 I_{pc}} \left(0.039 k \pi^2 + 2 \sqrt{\frac{(\Gamma + a^2 I_y)C}{E}} \right)$$

One may note that, as in the case of isotropic plate buckling, the critical stress obtained by using the above expression is independent of both the span and the number of half waves.

Assume that the shear center S for the stiffener is located at its centroid, O (see Fig. 18). The following stiffener properties may then be calculated. Note that d, t, and b are the pertinent depth, thickness, and spacing, respectively.

$$I_y = \text{moment of inertia about the y axis} = 6.8 \text{ in}^4$$

$$k = \text{torsion constant} = \frac{1}{3} d t^3$$

$$= 27.46 \text{ in}^4$$

$$\Gamma = \text{warping constant} = \frac{t^3 b^3}{36}$$

$$= 1364 \text{ in}^4$$

$$C = \text{spring stiffness supplied by the plating [41, p.109]}$$

$$= \frac{E t^3}{3 b}$$

$$= 8.88 \times 10^5 \text{ lb-in/in}$$

$$I_{pc} = \text{polar moment of inertia about the enforced center of rotation } C_E$$

$$= 7275 \text{ in}^4$$

and hence,

$$r_e^2 = 14.04 \text{ in}^2 \text{ giving } \sigma_{TE} = 113 \text{ ksi} = 50.35 \text{ t/in}^2$$

For the inelastic range, using the expression given before, one obtains:

$$\sigma_T = 31.44 \text{ ksi} = 14.04 \text{ t/in}^2 = 0.93 \sigma_y$$

The longitudinal deck girder. The section properties are as given below (see Fig. 19):

$$a = \text{distance from } C_E \text{ to shear center}$$

$$= 31.45'' \text{ assuming that the shear center } S \text{ coincides with the centroid } O.$$

$$k \approx \frac{1}{3} \sum d t^3 = 2.82 \text{ in}^4$$

$$r \approx \frac{1}{36} \sum t^3 b^3 = 820.34 \text{ in}^6$$

$$C = \frac{E t^3}{3 b} = 2.96 \times 10^5 \text{ lb-in/in}$$

$$I_y = 47.18 \text{ in}^4$$

$$I_{pc} = 39.38 \text{ in}^4$$

Hence,

$$\min r_e^2 = 4.24 \text{ in}^2 \text{ and}$$

$$\sigma_{TE} = 34 \text{ ksi} = 15.2 \text{ t/in}^2$$

For the inelastic case we thus have $\sigma_T = 25.5 \text{ ksi} = 0.75 \sigma_y$, using the plasticity reduction-factor approach.

Unfortunately, the details and locations of the tripping brackets along the deep girder are not available. However, in a girder such as this, the possibility of tripping collapse can be avoided to a considerable extent by the proper placement of such lateral support brackets which will be the case assumed in this analysis.

c. Grillage Failure Mode

i. Buckling of a Sub-Panel of the Grillage with Two Equidistant Flat-Bar Stiffeners

Following the analysis given in [24, p. 371], we obtain, for the case of simply supported boundary conditions (Figure 15):

δ = ratio of the cross section area of one stiffener to the area bt of the plate = 0.21.

γ = the ratio of flexural rigidity of one stiffener to that of the plate of width b

$$= \frac{E I}{b D} = 51.60 \text{ where,}$$

D = the flexural rigidity per unit width of the plate given by $\frac{E t^3}{12(1-\nu^2)}$

The buckling form is determined by a parameter:

$$\begin{aligned}\gamma_0 &= 14.5 \sqrt{\alpha^3} + 36 \alpha^2 \delta \\ &= 32.3 \text{ in this case.}\end{aligned}$$

Since $\gamma > \gamma_0$ here, the panel buckles in an antisymmetrical mode with the stiffeners forming rigid nodal lines. The elastic critical stress is the same as the isotropic plate buckling stress in this case.

$$\sigma_c = 169 \text{ ksi} = 75 \text{ t/in}^2$$

In the inelastic range, failure occurs by the elastoplastic yield of the flat-bar stiffeners. Both the flexural and tripping failure stresses for this mode have been previously obtained.

ii. Overall Grillage Instability

In this mode of failure, the entire grillage together with all constituent stiffening, buckles over its length into one or more half waves. Column failure would usually precede this mode of failure except in very slender grillages. Grillage failure would presumably be affected by the tripping of girders. The following analysis does not account for that interaction. The effect due to edge shear is also neglected.

The elastic buckling stress (σ_{GE}). Under uniaxial compression in the z direction, the critical stress is given by orthotropic plate theory [7, p. 32]:

$$\sigma_{GE} = \frac{k \pi^2 \sqrt{D_z D_x}}{t_z b^2}$$

where

$$k = \frac{m^2}{p^2} + 2\eta + \frac{p^2}{m^2} \quad \text{for the simply supported case}$$

$$p = \text{the virtual aspect ratio} \equiv \frac{a}{b} \sqrt{4 \frac{D_x}{D_z}}$$

a, b = the gross panel length (z direction) and the breadth (x direction) respectively

m = the number of half waves in which the gross panel buckles along the z direction

D_z, D_x = the flexural rigidities per unit width of the material along the z and x directions, respectively

D_{zx} = the twisting rigidity per unit width

t_z = an average cross-sectional area per unit width of effective plating and stiffeners in the z direction

The properties relevant to the application of orthotropic plate theory are now given for the $m=1$ case:

$$D_z = \frac{E_z t^3}{12(1-\nu_z \nu_x)} = \frac{E_z i}{1-\nu_z \nu_x}$$

where i is the moment of inertia per unit width of the orthotropic plate, and

$$= \frac{E I_z}{S(1-\nu^2)}$$

where S is the stiffener spacing and I_z is the moment of inertia of the stiffener and an effective width of plating in the z direction.

With $I_z = 18838 \text{ in}^4$, $\nu = 0.3$, and $S = 114 \text{ in.}$, we have:

$$D_z = 5.45 \times 10^9 \text{ lb-in/in}$$

$$D_x = \frac{E h^3}{12(1-\nu^2)} = 9.27 \times 10^6 \text{ lb-in/in}$$

$$\frac{D_{zx}}{\sqrt{D_z D_x}} \cong \text{torsion coefficient } \eta = \sqrt{\frac{I_{pz} I_{px}}{I_z I_x}} = 0.602$$

I_p = the moment of inertia of the plate alone about the neutral axis of the plate stiffener combination.

Hence,

$$D_{zx} = 1.353 \times 10^8 \text{ lb-in/in}$$

$$p = 0.085$$

$$k = 138.6$$

$$t_z = 1.584''$$

From these parameters the elastic critical stress was found to be very high and thus, this mode is not a governing mode of failure in this case.

3. Evaluation of the Governing Mode of Failure and Estimation of the Ultimate Strength of the Hull

a. The Moment Initiating Yield

The moment initiating yield in the deck gross panel is given by:

$$M_i = SMe \times \sigma_y$$

where,

$$\begin{aligned} SMe &= \text{the conventional elastic section modulus} \\ &= 4.043 \times 10^5 \text{ in}^2\text{-ft.} \end{aligned}$$

and

$$\begin{aligned} \sigma_y &= \text{the yield stress of the material} \\ &= 34 \text{ ksi} = 15.18 \text{ t/in}^2 \end{aligned}$$

We thus have:

$$M_i = 6.14 \times 10^6 \text{ ft-tons} \quad (74)$$

Note that this computation assumes that the structural elements constituting the section remain stable throughout the entire range of load application.

b. The Ultimate Strength Including Instability Modes of Failure

We may now calculate the ultimate load carrying capacity of the hull girder in longitudinal bending. If we assume that failure in the deck occurs at a stress equal in magnitude to $\phi \sigma_y$, where ϕ is a structural instability factor introduced in order to account for the buckling failure of the structure at deck, we then have the ultimate moment given by:

$$M_u = \phi \times SMe \times \sigma_y$$

If we assume that the deeper deck longitudinals have been sufficiently strengthened against tripping, the structural instability factor for our case is then determined by the tripping of the flat-bar stiffeners. With $\phi = 0.93$, we may then obtain the ultimate vertical bending moment as:

$$M_u = 5.71 \times 10^6 \text{ ft-tons} \quad (75)$$

c. The Ultimate Strength Due to Yielding and Plastic Flow

The vertical fully plastic yield moment was calculated in subsection 1 of this section, including the combined effects of the lateral and torsional moments, to be:

$$M_x = 6.157 \times 10^6 \text{ ft-ton} \quad (76)$$

Comparing Equations (74), (75), and (76), it is clear that the governing failure mode is that due to instability of deck longitudinals and the estimated ultimate moment in this case is 5.7×10^6 ft-ton.

It should be noted that Caldwell's [2] approach for including buckling modes of failure in the fully plastic moment analysis (i.e., using the plastic collapse moment formulation) gives a more optimistic value of the ultimate strength. In separate calculations conducted under this study, his approach yielded an ultimate strength value of 6.46×10^6 ft-ton including buckling effects, but excluding lateral and torsional moment effects.

VI. CONCLUSIONS AND RECOMMENDATIONS

Although some of the ultimate modes of failure of a hull girder can be analyzed with some degree of confidence, others are far from being well established or completely reliable. Those failure modes which need particular attention are usually the ones which involve coupling between several mechanisms of failure. Therefore, additional analytical work as well as experimental verification programs are necessary. These two aspects of our recommendations are discussed in the following paragraphs.

A. Analytical and Semi-Emperical Work

1. The torsion mode of hull failure in association with open-deck vessels such as containerships needs further investigation. Although this mode of failure was not found to be important and has little or no effect on the fully plastic moment and other collapse modes of full-deck vessels, the situation can be different in open-deck vessels and should be thoroughly examined.

2. The hull modes of failure should be further investigated when coupling occurs between two or more mechanisms of failure, e.g., plate buckling occurring simultaneously with instability of stiffeners and plastic yielding.

3. Further attention should be given to hull failure resulting from stiffeners tripping, i.e., lateral-torsional buckling. The inelastic tripping of stiffeners welded to continuous plating and the appropriate location of tripping brackets require further examination.

4. In the shakedown analysis, the probability of occurrence of several loads which cause plastic flow in the hull girder over its lifetime is very important. If these loads do not occur more than once or twice in the lifetime, then shakedown analysis is not necessary and can be ignored as one of the hull girder modes of failure. On the other hand, if these loads are expected to occur several times during the hull life, shakedown analysis can be important and should be examined as a possible failure mode. Therefore, an investigation of the expected probability of occurrence of such loads which lead to plastic flow in the hull is needed.

5. An investigation, similar in scope to this study but with attention focussed on the fracture modes of failure, is recommended. At present, a separate analysis must be carried out for cumulative damage by fatigue when conditions are conducive to this type of failure. Both fatigue and fracture modes of hull failure should be further developed and incorporated in a general analysis procedure together with the other modes of failure discussed in this report. This is important because the final failure of the hull may occur prematurely under the single application of an "ultimate" bending moment if the momentarily existing carrying capacity of the hull is somewhat reduced by fatigue to the extent that it cannot sustain this moment. Local weakness, particularly at the joints and structural connections, should be included in such a study.

B. Experimental Program for Verification

As has been pointed out earlier, some of the expressions and formulations for estimating the collapse load of a hull girder are not well established and a need for further verification exists. An experimental program may not provide all answers to the questions raised, but, without doubt, it will provide insight into some of the difficult problems and possibly a measure for determining the relative reliability of the different analytical formulations. It is envisioned that two groups of experimental programs fulfilling two complementary objectives will provide the maximum benefits. The two groups are:

1. Group A

Objective:

To verify and calibrate the recommended methods and procedures for predicting the ultimate strength and collapse moments of a hull girder under vertical and combined moments through correlations and comparisons with experimental results.

Plan:

Relatively small-scale models (6 to 8 ft. in length) should be sufficient in this regard. The breadth-to-depth ratio of the models should be within the same range of values as those of actual ships. The end sections of the model (about 2 ft. in length) should be sufficiently strong to avoid premature failure in those regions. The middle section of the model which is the "test specimen" (about 2 to 4 ft. in length) should be designed to be interchangeable. In this manner, the test facilities and end sections can be suitable for accommodating several middle sections designed to fail in different modes of failure. For example, some of the middle sections may be designed to fail by instability of longitudinal stiffeners or overall grillage instability, while others may be designed to accommodate a moment equal to the fully plastic moment prior to any grillage instability.

The support system and external loads should be applied only at the end sections of the model. The external loads can be designed such as to produce vertical moment only or vertical moment and torque or, by applying the loads diagonally on the end sections combined vertical, lateral, and torsional moments can be induced.

Properties of the materials used in the construction of the models should be tested in tension and compression. Initial deformation due to welding distortions and plate unfairness should be measured and recorded prior to testing. Deflection and strain measurements should be taken through the elastic and plastic ranges up to the collapse loads. Stages of development of each failure mode should be observed and recorded together with the corresponding collapse load.

The previous experimental work sponsored by the Ship Structure Committee [9,10,11] fits and contributes to this group.

2. Group B

Objective:

To examine the likelihood of different modes of failure in models large enough to allow for reliable extrapolation of the results to actual ship sizes.

Plan:

This is envisioned as a long-term phase which involves relatively large models (about 40 ft. in length). The models should be scaled accurately to represent actual ships. Two strong end sections with an interchangeable middle section as in Group A can be used also here. Since the middle section is a large-scale model of an actual ship, the likely modes of failure can be examined and the corresponding collapse loads can be extrapolated to the full size. The effects of residual stresses and welding distortions on the collapse moment can be realistically examined. In addition, the tests should provide results which can be used for further verification or modification of the recommended analytical formulations and the development of new empirical expressions. Testing facilities such as existing at David Taylor Naval Ship Research and Development Center and at the University of California, Berkeley, are suitable for such large-size experiments.

ACKNOWLEDGEMENT

The authors are grateful to the Ship Structure Committee for supporting this study, and to the program advisory committee members for their comments and discussion. Sincere thanks are expressed to Ms. S. Monrad for her work on the manuscript.

REFERENCES

- [1] International Ship Structures Congress, Report of Committee 10, Proceedings, Volume 2, 1967.
- [2] Caldwell, J.B., "Ultimate Longitudinal Strength," Transactions, Royal Institution of Naval Architects, Vol. 107, 1965.
- [3] Faulkner, D., Written discussion to reference (1).
- [4] Betts, C.V. and Attwell, D.M., "The Ultimate Longitudinal Strength of Ships," Shipbuilding and Shipping Record, December 30, 1965, p. 889.
- [5] "Report of Committee on Plastic and Limit Analysis," International Ship Structures Congress, Tokyo, 1970.
- [6] Evans, J.H. (editor), "Ship Structural Design Concepts," SSC, Project SR-200, U.S. Coast Guard, Washington, D.C., 1974.
- [7] Mansour, A.E., "Gross Panel Strength Under Combined Loading," Ship Structures Committee Report, SSC-270, 1977.
- [8] Schultz, H.G., "Buckling and Post-buckling of a Transversely Stiffened Ship Hull Model," Journal of Ship Research, SNAME, 1964.
- [9] Becker, H., "Feasibility Study of Model Tests of Ship Hull Girders," Ship Structure Committee Report, SSC-194, 1969.
- [10] Becker, H., "Compressive Strength of Ship Hull Girders," Part I, SSC-217, 1970 and Part II, SSC-223, 1971.
- [11] Clarkson, J., "A Survey of Some Recent British Work of the Behavior of Warship Structures," SSC-178, November 1966.
- [12] Sugimura, T., Nozaki, S., and Suzuki, T., "Destructive Experiment of Ship Hull Model Under Longitudinal Bending," Journal SNA, Japan, Vol. 119, June 1966.
- [13] Stiansen, S.G., Mansour, A., Jan, H.Y., and Thayamballi, A., "Reliability Methods in Ship Structures," Royal Institution of Naval Architects, Spring Meeting, 1979.
- [14] Hodge, P.G., "Plastic Analysis of Structure," McGraw Hill, 1959.
- [15] Mansour, A., "Charts for the Buckling and Post-buckling Analyses of Stiffened Plates Under Combined Loading," Technical and Research Bulletin No. 2-22, Society of Naval Architects and Marine Engineers, July 1976.
- [16] Timoshenko and Gere, "Theory of Elastic Stability," Second Edition, McGraw-Hill Book Company, 1961.
- [17] Faulkner, D., "A Review of Effective Plating for Use in the Analysis of Stiffened Plating in Bending and Compression," Journal of Ship Research, March 1975.

- [18] Mansour, A., "Postbuckling Behavior of Stiffened Plates with Small Initial Curvature under Combined Loads," International Shipbuilding Progress, June 1971.
- [19] Schultz, H.-G., "Recent Development in Ship Hull Girder Investigations," Paper presented at SNAME Northern California Section, March 1964.
- [20] Faulkner, D., "The Overall Compression Buckling of Partially Constrained Ship Grillages," M.I.T., 1973.
- [21] Smith, C.S., "Compressive Strength of Welded Steel Ship Grillages," RINA Spring Meeting, 1975.
- [22] Terazawa, K., et.al., "Analysis of Elastic-Plastic Buckling of Plates with Stiffeners by Finite Element Method," Selected papers from the Journal of the Society of Naval Architects of Japan, Vol. 127, 1970.
- [23] Kondo, J., "Ultimate Strength of Longitudinally Stiffened Plate Panels Subjected to Combined Axial and Lateral Loading," Fritz Laboratory Report No. 248.13, Lehigh University, August 1965.
- [24] Bleich, F., "Buckling Strength of Metal Structures," McGraw-Hill Book Company, New York, 1952.
- [25] Smith, C.S., Kirkwood, W.C., and McKeeman, J.L., "Evaluation of Ultimate Longitudinal Strength of a Ship's Hull," R671, Admiralty Marine Technology Establishment, 1977.
- [26] Mansour, A., "Ship Bottom Structure under Uniform Lateral and Inplane Loads," Schiff und Hafen, Heft 5, 1967.
- [27] Schultz, H.-G., "Zum Stabilitätsproblem Elastisch Eingespannter Orthotroper Platten," Schiff und Hafen, Heft 6, 1962.
- [28] Mansour, A., "Orthotropic Bending of Ship Hull Bottom Plating Under the Combined Action of Lateral and Inplane Loads," Published for MARAD as Report No. NA-66-2, Contract No. NA 2620, University of California, College of Engineering, Berkeley, 1966.
- [29] Numata, E., "Longitudinal Bending and Torsional Moments Acting on a Ship Model at Oblique Heading to Waves," Journal Ship Res., June 1960.
- [30] "S.S. Ocean Vulcan Sea Trials," Report No. R8, The Admiralty Ship Committee, 1953.
- [31] Comstock, J.P.(editor), "Principles of Naval Architecture," The Society of Naval Architects and Marine Engineers, New York, 1967.
- [32] D'Arcangelo, A.M. (editor), "Ship Design and Construction," The Society of Naval Architects and Marine Engineers, New York, 1969.
- [33] Payer, H.-G., "Notes on the Buckling and Post-buckling Behaviour of Deep Web Frames," J. Marine Tech., July 1972.

- [34] Timoshenko, S., "Stability of Rectangular Plates with Stiffeners," Mem. Inst. Engrs. Ways of Commun., Vol. 89, 1915 (in Russian).
- [35] Wang, T.-K., "Buckling of Transverse Stiffened Plates Under Shear," J. Applied Mechanics, Vol. 14, 1947.
- [36] Stein, M. and Fralich, R.W., "Critical Shear Stress of Infinitely Long Simply Supported Plate with Transverse Stiffeners," NACA Tech. Note, 1851, 1949.
- [37] Hill, R., "A Variational Principle of Maximum Plastic Work in Classical Plasticity," Quarterly J. Mech. Appl. Math., 1, 18-28 (1948).
- [38] Hill, R. and Siebel, M., "On the Plastic Distortion of Solid Bars by combined Bending and Twisting," J. Mech. & Phys. Solids, 1, 1953.
- [39] Mansour, A., "On the Nonlinear Theory of Orthotropic Plates," Journal of Ship Research, December 1971, p. 266.
- [40] Horne, M.R., "Plastic Theory of Structures," The M.I.T. Press, Cambridge, Mass., 1971.
- [41] Faulkner, D., "Compression Strength and Chance," Defense Fellowship Thesis, Mass. Institute of Technology, Cambridge, 1972.
- [42] Schade, H.A., "The Effective Breadth of Stiffened Plating Under Bending Loads," Trans. SNAME, Vol. 59, 1951.
- [43] Schade, H.A., "The Effective Breadth Concept in Ship Structure Design," Trans. SNAME, Vol. 61, 1953.
- [44] Jones, N., "On the Shakedown Limit of a Ship's Hull Girder," Journal of Ship Research, Vol. 19, No. 2, June, 1975.

APPENDIX I

CRITERIA FOR YIELD UNDER COMBINED STRESSES

The response of structural elements to uniaxial stress or pure shear can be represented by stress-strain diagrams that may be used to predict the onset of yield directly using material properties derived from analogous laboratory tests. Practical structures, however, are subjected to loads that give rise to combined multiaxial stress distributions. In order to apply plastic theory, one now is faced with the necessity of having to define yield point under a multiaxial state of stress. The two most common theories for accomplishing this quantitatively are the Maximum Shear Stress Theory and the Maximum Distortion Energy Theory. Both are discussed here for the case of the biaxial stress.

1. The Maximum Shear Stress Theory

This theory usually bears the name of H. Tresca (1868). In laboratory specimen under a uniaxial loading, it may be observed that slippage occurs along planes of maximum shear stress during yield. This theory uses the same criterion under combined stress; the onset of yield is then taken to depend on the maximum shear stress attained. The critical value of stress is normally taken as the shear stress at yield in simple compression or tension. This may be obtained from the Mohr's circle of stress as:

$$\tau_{\max} \equiv \tau_{CR} = \sigma_{yp}/2$$

For the biaxial stress state with principal stresses σ_1 and σ_2 , we then have yield governed by the criterion:

$$\tau_{\max} = \frac{1}{2} \left| \frac{\sigma_1 - \sigma_2}{2} \right| \leq \frac{\sigma_{yp}}{2}$$

This yield criterion is often represented by the hexagon in Figure 20. Each point on the boundary represents a limiting state of biaxial stress. Points inside the hexagon indicate elastic behaviour. The concept of a yield stress is then replaced by the concept of a yield curve or surface.

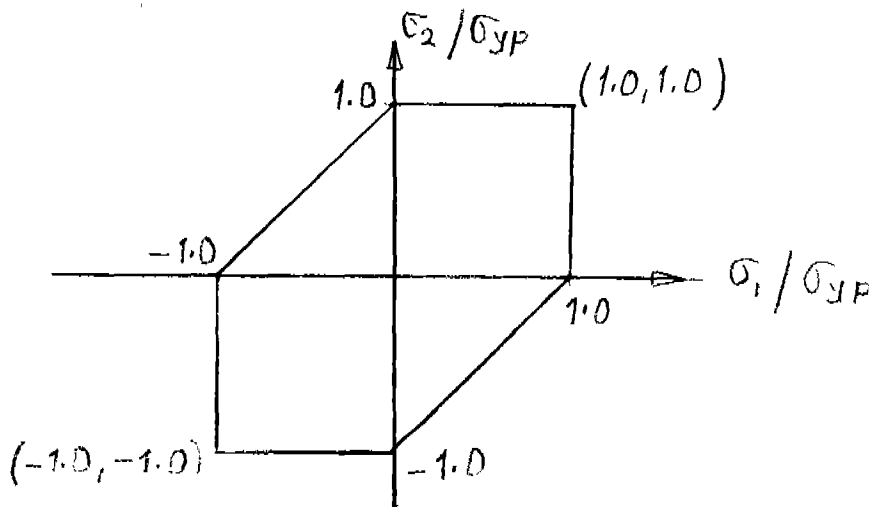


FIGURE 20. Tresca Yield Surface

2. The Maximum Distortion Energy Theory

This is the other widely used yield criterion for ductile isotropic materials. In its present form, the theory was proposed and explained by M.T. Huber (1904), R. von Mises (1913), and H. Hencky (1925). This approach visualizes the total elastic energy as consisting of a part associated with volumetric changes in the material, and the other causing shear distortions. The shear-distortion energy under the combined stresses is equated to that under simple tension at yield point in order to establish the yield criterion. The interested reader may refer to [1] for details. The basic law for the ideally plastic material under a plane stress is given for this case in terms of the principal stresses σ_1 and σ_2 as:

$$\sigma_1^2 + \sigma_2^2 - \sigma_1 \sigma_2 = \sigma_{yp}^2$$

This criterion may be represented by the ellipse shown. Points contained within the ellipse indicate elastic behaviour. The ellipse represents the yield surface as shown in Figure 21:

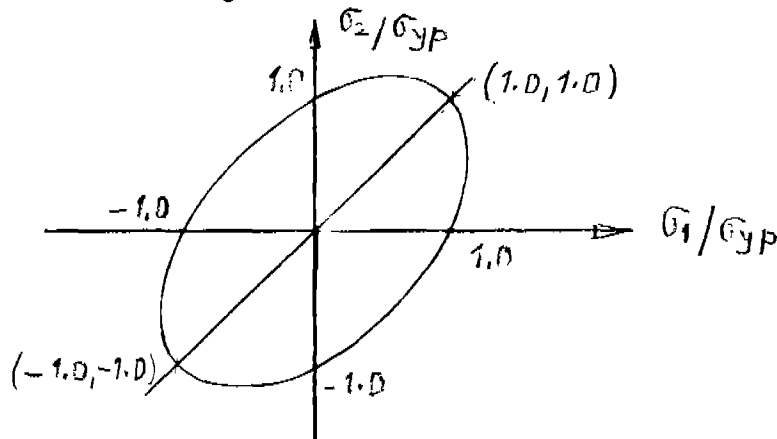


FIGURE 21. Von Mises Yield Surface

The von Mises criterion is also sometimes referred to as the octahedral shear stress criterion. It closely approximates the Tresca hexagon for the biaxial stress state, but has the additional advantage of being a continuous function. Note that both the theories presented apply to ductile materials exhibiting isotropic behaviour. Additionally, they assume properties identical in tension and compression.

3. An Example: Combined Shear and Bending of Beams

Consider the beam with its axis oriented along the z direction, as shown in Figure 22:

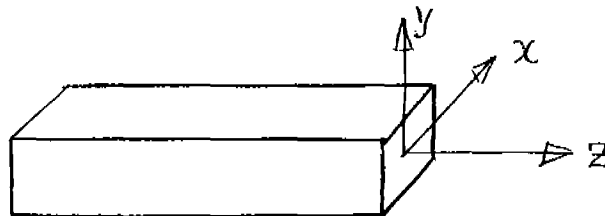


FIGURE 22. Box Beam Coordinates

The beam may be considered symmetrical about the y-z plane. The components specifying the stress state here are:

$$\sigma_z = \sigma$$

and

$$\tau_{yz} = \tau$$

τ_{xz} may be neglected because of the symmetry assumed.

The Tresca yield condition states that the maximum shear stress should equal half the yield stress in simple tension for an element to be plastic. Here the principal stresses are given by:

$$\sigma_{1,2} = \frac{\sigma}{2} \pm \sqrt{\left(\frac{\sigma}{2}\right)^2 + \tau^2}$$

Hence the Tresca condition for this case is:

$$\tau_{\max} = \pm \left| \frac{\sigma_1 - \sigma_2}{2} \right| = \pm \sqrt{\left(\frac{\sigma}{2}\right)^2 + \tau^2} \leq \frac{\sigma_{yp}}{2}$$

This simplifies to:

$$\sigma^2 + 4 \tau^2 = \sigma_{yp}^2$$

The von Mises yield condition for the same case is obtained from:

$$\sigma_1^2 + \sigma_2^2 - \sigma_1 \sigma_2 = \sigma_{yp}^2$$

On substituting for σ_1 and σ_2 , one may obtain for the yield curve:

$$\sigma^2 + 3 \tau^2 = \sigma_{yp}^2$$

Note that in this case, we may recast the results into one convenient form:

$$\sigma^2 + \beta^2 \tau^2 = \sigma_{yp}^2$$

where

$$\beta = 2 \text{ (Tresca)}$$

$$= \sqrt{3} \text{ (von Mises)}$$

This expression is readily reduced to the case of pure tension or pure shear by setting the appropriate terms to zero.

APPENDIX II

THEOREMS OF LIMIT ANALYSIS

Consider the behaviour of a general structure under the action of an arbitrary set of loads that are in equilibrium. For the present, assume that the structure is made up of a rigid perfectly plastic material. The load for which the structure remains in equilibrium, but does not remain rigid, with the displacements increasing indefinitely, is variously called the limit load, the fully plastic yield load, or the collapse load. The theorems of limit analysis aim at determining that load. The extent of generality of these theorems is discussed later.

1. The Static or the Lower Bound Theorem

If it is possible to find a stress distribution over the entire structure that is in equilibrium with the external applied loads and is everywhere below or at yield, the structure will not collapse or will just be at the verge of collapse. This theorem yields a load from static considerations which is less than or equal to the failure load, and thus gives a lower bound on the collapse load.

2. The Kinematic or the Upper Bound Theorem

If there exists any compatible pattern of plastic mechanism deformations for which the rate at which the external forces do work exceeds the rate of internal dissipation, the structure will collapse. The associated load given from kinematic considerations will be greater than or equal to the load at failure. We thus have an upper bound on the collapse load.

This theorem states that if a path to failure exists, the structure will not stand up. For practical purposes, these two theorems would enable bracketing the collapse load. A unique collapse load does exist. It may be defined as one where the resulting stress distribution is in equilibrium with the external loads, nowhere exceeds the yield stress, and simultaneously transforms the structure into a mechanism with yield hinges at a sufficient number of locations.

In the context of the above state theorems, the collapse load is the one that is the highest obtained from statics and the lowest obtained from kinematics. For a proof of the above theorems, one may refer to [14; pp. 201-205].

The theorems are valid for any combination of external loads, e.g., combined bending, axial, and torsional loads. Even though proportional loading is usually assumed in describing these theorems in terms of load factor, any set of proportional or non-proportional loading may occur. The structure will collapse at the first combination of loads whose stress distribution satisfies the conditions of equilibrium, mechanism and yield [40]. Thus the stress distribution over the structure at collapse is not unique. The collapse load, however, is unique.

The general validity of this approach to a structure of a given material depends on the material's behaviour when loaded. The stress-strain curves for mild steel make it a good candidate for the application of plastic theory. One may also note here that the assumption of rigid plasticity, with an infinite elastic modulus, though conceptually simpler, may be replaced by that of elastic-perfect plasticity with a finite elastic modulus. The collapse load is independent of the Young's modulus. A restriction in doing so is that the changes in geometry due to the resulting elastic deflections should be small enough to be neglected.

SHIP RESEARCH COMMITTEE
Maritime Transportation Research Board
National Academy of Sciences-National Research Council

The Ship Research Committee has technical cognizance of the interagency Ship Structure Committee's research program:

Mr. O. H. Oakley, Chairman, Consultant, McLean, VA
Prof. A. H.-S. Ang, University of Illinois, IL
Mr. M. D. Burkhart, Consultant, Clinton, MD
Dr. J. N. Cordea, Senior Staff Metallurgist, ARMCO INC., Middletown, OH
Mr. D. P. Courtsal, Vice President, DRACO Corporation, Pittsburgh, PA
Mr. W. J. Lane, Consultant, Baltimore, MD
Mr. A. C. McClure, Alan C. McClure Associates, Inc., Houston, TX
Dr. W. R. Porter, Vice Pres. for Academic Affairs, State Univ. of N.Y.
Maritime College
Prof. H. E. Sheets, Director of Engineering, Analysis & Technology, Inc.,
North Stonington, CT

The Ship Design, Response, and Load Criteria Advisory Group prepared the project prospectus, evaluated the proposals for this project, provided the liaison technical guidance, and reviewed the project reports with the investigator:

Mr. W. J. Lane, Chairman, Consultant, Baltimore, MD
Mr. J. W. Boylston, Manager, Marine Operations, El Paso Marine Company
Solomons, MD
Prof. J.-N. Yang, Department of Civil, Mechanical & Environmental Engineering,
George Washington University, Washington, DC
Mr. L. R. Glostén, L. R. Glostén Associates, Inc., Seattle, WA
Mr. P. M. Kimon, EXXON International Company, Florham Park, NJ
Dr. O. H. Oakley, Jr., Project Engineer, GULF R&D Company, Houston, TX
Mr. J. E. Steele, Naval Architect, Quakertown, PA

SHIP STRUCTURE COMMITTEE PUBLICATIONS

These documents are distributed by the National Technical Information Service, Springfield, VA 22314. These documents have been announced in the Clearinghouse Journal U. S. Government Research & Development Reports (USGRDR) under the indicated AD numbers.

- SSC-285, *Critical Evaluation of Low-Energy Ship Collision-Damage Theories and Design Methodologies - Volume I - Evaluation and Recommendations* by P. R. Van Mater, Jr., and J. G. Giannotti. 1979. AD-A070567.
- SSC-286, *Results of the First Five "Data Years" of Extreme Stress Scratch Gauge Data Collection Aboard Sea-Land's SL-7's* by R. A. Fain and E. T. Booth. 1979. AD-A072945.
- SSC-287, *Examination of Service and Stress Data of Three Ships for Development of Hull Girder Load Criteria* by J. F. Dalzell, N. M. Maniar, and M. W. Hsu. 1979. AD-A072910.
- SSC-288, *The Effects of Varying Ship Hull Proportions and Hull Materials on Hull Flexibility Bending and Vibratory Stresses* by P. Y. Chang. 1979. AD-A075477.
- SSC-289, *A Method for Economic Trade-Offs of Alternate Ship Structural Materials* by C. R. Jordan, J. B. Montgomery, R. P. Krumpen, and D. J. Woodley. 1979. AD-A075457.
- SSC-290, *Significance and Control of Lamellar Tearing of Steel Plate in the Shipbuilding Industry* by J. Sommella. 1979. AD-A075473.
- SSC-291, *A Design Procedure for Minimizing Propeller-Induced Vibration in Hull Structural Elements* by O. H. Burnside, D. D. Kana, and F. E. Reed. 1979. AD-A079443.
- SSC-292, *Report on Ship Vibration Symposium '78 - Sheraton National Hotel, Arlington, VA.* by E. Scott Dillon. 1979. AD-A079291.
- SSC-293, *Underwater Nondestructive Testing of Ship Hull Welds* by R. Youshaw and C. Dyer. 1979. AD-A079445.
- SSC-294, *Further Survey of Inservice Performance of Structural Details* by C. R. Jordan and L. T. Knight. 1979.
- SSC-295, *Nondestructive Inspection of Longitudinal Stiffener Butt Welds in Commercial Vessels* by R. A. Youshaw. 1980.
- SSC-296, *Review of Fillet Weld Strength Parameters for Shipbuilding* by C-L Tsai, K. Itoga, A. P. Malliris, W. C. McCabe, and K. Masubuchi. 1980.
- SSC-297, *Evaluation of Liquid Dynamic Loads in Slack LNG Cargo Tanks* by P. A. Cox, E. B. Bowles, and R. L. Bass. 1980.
- SSC-298, *Investigation of Steels for Improved Weldability in Ship Construction - Phase I* by R. W. Vanderbeck. 1980.